Origin and Emplacement Mechanisms of the Slieve Gullion Ring Dyke Complex, Ireland

Heather Graham

A thesis submitted in partial fulfilment of the requirements of Liverpool John Moores University for the degree of Master of Philosophy

This research programme was carried out in collaboration with Mourne Cooley Gullion Geotourism

March 2016

Contents

List of figures

List of tables

Abstract

The purpose of this research was to study the rock units of the Slieve Gullion ring dyke complex, to determine their composition, structure and position within the stratigraphic sequence; as well as producing a model for the emplacement of these units. A combination of detailed field observations, mapping, rock sample collection and structural measurements were obtained at selected field sites around the ring dyke complex. In the laboratory, the rock samples obtained were prepared for thin section and geochemical analysis. When compared to previously published geochemical data, the results found here were generally in agreement. The geochemistry results obtained for the various rock units studied were also generally within the expected igneous rock categories on the IUGS classification graph. There are some exceptions to this however and it is suggested here that those rocks have undergone hydrothermal secondary alteration, which is supported by the presence of infilled fractures within the outcrops and evidence for the presence of hot fluids (tuffisites). The geochemistry data plots all of the rocks studied here (apart from the basalts) within the alkaline or high-k calc-alkaline series on the tectonic environment graph of Ewart (1982). This suggests a cratonic or continental rift environment which supports that this igneous complex is related to the opening of the Atlantic Ocean. The geochemistry results and observations of the thin sections for the rafts of basalt found within the Forkill Quarry both confirm that these outcrops are basalts. It was also found that the basalts were geochemically similar to the Antrim basalts and it is therefore suggested here that the Forkill Quarry basalts predate the formation of the ring dyke. Overall this research agrees with the traditional ring dyke emplacement model as proposed by Emeleus et al. (2012) due to the presence of multiple sharp contacts between the rock units as well as evidence of crushing and the presence of percolating hot fluids near to rock contacts.

1. Introduction

The Slieve Gullion Ring Dyke Complex has been the focus of several studies most of which look at the petrology and geochemistry of rock units within the complex (Patterson, 1952/53; Richey, 1932; Emeleus, 1961-63; Gamble, 1982). There are also several studies (Gamble, 1979; Gamble et al. 1992) that focus on the central sheeted unit within the complex. However due to political conflicts little research has been done since the 1960's. What little research there is highlights a debate over how the complex was emplaced i.e. traditional ring dyke emplacement (Emeleus et al. 2012) or some form of sill emplacement (Stevenson et al. 2008). The aim of this study is therefore to re-evaluate the Slieve Gullion ring dyke emplacement models and to understand the igneous processes that occurred during ring dyke formation. The objectives of this study are: 1) To study in detail, the igneous rock units present in the ring complex, to determine their composition, structure and position in the stratigraphic sequence; This includes: a) Forkill volcanic breccias, b) porphyritic rhyolite and c) newly discovered outcrops of the basalt unit in the Forkill Quarry; and 2) To produce a model for the emplacement of different rock units within the Slieve Gullion ring complex.

2. Geological setting and geological history of the North Atlantic Igneous Province

The North Atlantic Igneous Province (NAIP) covers a large area that includes Baffin Island, Greenland, Iceland, the Faeroe Islands, Northeast Ireland and northwest Britain (Hitchen and Ritchie, 1993). It is thought that the NAIP developed due to the breakup of Euramerica, that is, when the North American plate rifted from the Eurasian plate. The igneous activity is thought to have been due to what is now known as the Iceland Mantle Plume, interacting with the Mid-Atlantic rift zone (Meade et al. 2009). The Iceland Plume was once beneath Greenland and it is thought that the rising magma from this plume facilitated the development of igneous centres and was followed by the opening of the North Atlantic Ocean (Cooper et al. 2012). White (1988) also suggests that the activity that occurred during the opening of the North Atlantic Ocean can be explained by a mantle hot spot, which seems to fit the Iceland Plume theory. White (1988) further suggests that this hotspot would explain the distribution, volume and rapid production of the large amount of igneous rocks found. At present this plume lies beneath Iceland, hence 'Iceland Plume', and it is thought to be producing new crust in excess of 15km thick. There is a trace of the movement caused by the opening of the North Atlantic, shown by the Greenland-Faeroe ridge (White, 1988). Volcanism within the NAIP is thought to have occurred in two settings. The first being within the igneous provinces of NW Scotland, NE Ireland, the Faeroes and

Greenland; the second being subaqueous along the rifted margins on both sides of the North Atlantic Ocean (White, 1988).

Saunders et al (1997) suggests two main phases of activity within the NAIP. The first phase of activity is thought to have begun around 62 Ma and produced the thick lava flows that can be seen on the Hebridean Islands and at Antrim (N Ireland). The second phase of activity is thought to have begun around 56 Ma. Data published by Pearson et al (1996) provides dates for rock samples at the base of the phase 1 lava flows, giving ages of 62.8±0.6 and 62.4±0.6 Ma. These dates help to constrain the initiation of activity in the NAIP. These dates are also in agreement with Brooks (1973) who suggests an age of 60 Ma for the opening of the North Atlantic Ocean between Greenland and the Rockall Plateau and Cooper et al (2012) who suggest a date of approximately 55 Ma for the opening of the North Atlantic Ocean.

Within the NAIP there is an area known as the British and Irish Palaeogene Igneous Province (BIPIP). The BIPIP covers an area that is both on and offshore Britain (Hitchen and Ritchie, 1993), which is shown in Figure 1; and it includes multiple intrusive centres, lava fields and dyke swarms (Bell and Emeleus, 1988). The lava fields can be found on the Isle of Skye, the Isle of Mull, and Antrim, while the central complexes (intrusive centres) can be found in several locations including Skye, Mull, Rhum, Ardnamurchan, Arran, Mourne, Carlingford, Slieve Gullion, and several submerged locations offshore (Bell and Jolley, 1997). Geological maps of some of these complexes are shown in Figure 2, however other maps for various BIPIP complexes are available in Gelmacher et al (1998), Holness and Isherwood (2003), Meade et al (2009), Meighan et al (1984) and Le Bas (1966). Meighan et al (1992) also include Rockall and St Kilda in their list of BIPIP complexes and Thorpe et al (1990) include Lundy (located in the Bristol Channel) in the BIPIP as the southernmost igneous complex. Bell and Emeleus (1988) suggest that the majority of the complexes are located within a zone of crustal thinning that extends in an almost N-S line, and this general structural trend can be identified on Figure 1, which shows the location of the majority of the igneous complexes within the BIPIP.

Figure 1: Map showing the location of igneous complexes of the BIPIP, including the Slieve Gullion Complex (underlined in red). From Bell and Emeleus (1988).

Meade et al (2009) suggest that the BIPIP formed during the first phase of the NAIP, around 62 Ma. This is in general agreement with most published data as other scientists suggest dates of 62-58 Ma (Bell and Emeleus, 1988); 62-56 Ma (Gamble et al. 1999); 61-55 Ma (Meighan et al. 1992); and 60-50 Ma (Brooks, 1973) for the BIPIP. Within the BIPIP, each complex differs slightly in age. Table 1 shows a summary of published data for the onshore parts of the BIPIP from several scientists using several dating techniques (Rb-Sr, K-Ar, ^{40}Ar/^{39}Ar, U-Pb).

Hitchen and Ritchie (1993) provide a comprehensive summary detailing dates obtained for the offshore parts of the BPIP. The Faeroe-Shetland complex is thought to date to 52.9±1 to 83.5±5.2 Ma. They suggest dates of 46.1±2.7 to 62.4±1.3 Ma for the Hebrides shelf lavas; and 24.2±0.7 to 61.9±1.1 Ma for Rosemary Bank (Rockall Trough).

Most of these dates correspond with the overall dates for the BIPIP as a whole (62-50Ma); however, some of the offshore complexes are thought to be younger than the suggested dates for the whole province.

Figure 2: Geological maps of intrusive centres within the BIPIP (Walker, 1975).

Location	Suggested Age Range	Reference
Arran	61.7 to 57.4 Ma	Meade et al (2009)
Antrim	58 to 55 Ma	Bell and Jolley (1997)
	61±0.6 to 58.3±1.1 Ma	Wallace et al (1994)
	61 to 58 Ma	Cooper et al (2012)
	59.6 to 62.6Ma	Ganerod et al (2010)
Ardnamurchan	~60 Ma	Geldmacher et al (1998)
Mull	60 to 57 Ma	Dagley et al (1987)
Muck	63.1±2.3 Ma	Dagley and Mussett (1986)
Eigg	63.5±2 to 52 Ma	Dagley and Mussett (1986)
Rhum	60.53±0.8 Ma	Holness and Isherwood (2003)
Skye	59.3±0.7 to 58.7±1.7 Ma	Bell et al (1994)
Lundy	59-52 Ma	Smith and Roberts (1997)
	58.7±1.6 Ma	Thorpe et al (1990)
Carlingford	60.9±0.5 Ma	Gamble et al (1999)
Mourne	58±1.6 to 51.5±1.8[1] Ma	Gamble et al (1999)
	56 to 55 Ma	Cooper et al (2012)
	56.3±0.8 to 51.5±1.8 Ma	Wallace et al (1994)
Slieve Gulllion	58.5±2.3 to 57.6±1 Ma	Meighan et al (1988; cited in Gamble et al. 1992)
	58.5±2.3 to 56.5±1.3[12] Ma	Gamble et al (1999)
	57.6±1 Ma	Wallace et al (1994)

Table 1: A summary of published dates for locations in the BIPIP, based on length of activity and specific dates of units, obtained from various authors.

2.1 Ring dyke definitions

According to Troll et al (2005) a ring dyke is a circular intrusion that forms when magma rises along steep, outward dipping circular (or ring) fractures, and usually contains a central collapsed block. Richey's (1932) definition of a ring dyke is based on ring dykes found in Scotland (such as Mull and Ardnamurchan); a curve or ring shape dyke coupled with steep margins.

Kochar (1983) interprets ring dyke provinces as the continental location of mantle plumes/hot spots. The mantle plume is in a fixed location and moves through the plate producing igneous activity at the surface. Therefore, as the plate moves it changes the location of the activity on the surface. On oceanic plates this can form island chains, and on continental plates it forms alkaline magmatism, including sub-volcanic complexes.

It is thought that ring complexes provide an exposure of the magmatic plumbing beneath calderas and thus they can be used to reconstruct their geological history. Figure 3 shows a volcanic plumbing system, including a ring dyke/ring fault. Also the magma found within a ring dyke is a result of processes that occur within the magma chamber; as well as often being the result of caldera collapse (Kennedy and Stix, 2007). Marshall and Sparks (1984) suggest that central ring complexes provide an insight into magmatic evolution (such as magma mixing and differentiation), as they suggest that

often, the mixing of magmas with different compositions and temperatures occurs and produces mixed magma rocks and net-veined complexes.

Some caldera complexes are thought to have multiple (two or more) adjacent ring faults (Gudmundsson, 2007) which could provide the location for the development of multiple ring dykes.

Although ring faults/dykes are found at many extinct volcanoes, they are recognised at very few modern active locations. Several volcanoes are thought to have active ring faulting including; Sierra Negra and Fernandina (Galapagos); Rabaoul (Papau New Guinea); Campi Flegrei (Italy); Miyakejima (Japan); Dolomieu (La Reunion); Bardarbunga (Iceland); and Tendurek (Turkey); which may mean that these locations will be sites for future ring dykes (Bathke et al. 2013). It is also suggested that ring dyke provinces are indicators of future rift locations (Bonin, 1974; cited in Kochar, 1983).

Figure 3: Model of a volcanic plumbing system taken from Galland et al (2015).

2.2 Ring dykes around the world

There are numerous complexes around the world that contain one or more ring dykes. The Gardiner Complex in eastern Greenland is composed of concentric rings with a major ring dyke in the centre that is up to 400m wide and 2km in diameter (Neilsen and Buchardt, 1985). Neilsen and Buchardt (1985) interpret this ring dyke as a magma chamber which is supported by Neilsen (1980) who suggest that the rocks of this ring dyke have a magmatic origin which is indicated by structural and textural relationships, such as fine grained or chilled contacts. They further suggest that this complex is of Palaeogene age and is related to the opening of the North Atlantic, similar to those within the BIPIP.

Eklund and Shebanov (2005) draw attention to complexes located in Finland, specifically the Ava ring complex. They suggest that the Ava complex is one of three that is located in south-western Finland, along a north-east shear zone. The Ava complex is considered to be made up of hundreds of ring dykes of shoshonitic composition based on K_2O vs SiO_2 geochemical diagram of Peccerillo and Taylor (1976; cited in Eklund and Shebanov, 2005). The ring dyke is composed of K-feldspar granite occasionally mixed with shoshonitic monzonite.

The Gunninson annular complex, Colorado, consists of an inner ring of metamorphic rock and an outer ring of several tonalite and granodiorite intrusions which is thought to surround a central 'sill-like' diorite body (Lefrance and John, 2001).

The Meugueur-Meugueur ring structure in Niger is considered to be one of the largest in the world being 65km in diameter and around 200-300m wide. This complex also stands out petrographically as it is almost completely made up of a mildly alkaline melatroctolite or troctolite, with only minor inclusions of gabbro (Ritz et al. 1996).

Kochhar (1983) discusses the Tusham ring complex in India and suggest that the complex consists of granite outcrops and a quartz porphyry ring dyke. The ring dyke has an elliptical shape and is approximately 0.8/km in diameter. Kochhar (1983) suggests that this ring dyke can be explained by the mechanism of subsidence of a central block into the magma chamber. They suggest that there is a lack of flow structures and an undisturbed nature of the surrounding rock which can be considered to support the theory of subsidence mechanism. The lack of deformation to the surrounding rock is suggested to be the result of a fluid magma.

The Coldwell Alkaline Complex (Canada) consists of three overlapping ring dykes that show compositional differences which is thought to be due to multiple injections of magma. This is supported by the variable stratigraphy within the intrusions; the presence of xenolith rich horizons that separate distinctive layers/different lithologies; and the compositional variations of minerals

within the intrusion (Shaw, 1997). Shaw (1997) suggests that the first injection of magma cooled rapidly and as faulting continued more pulses of magma were emplaced which they suggest crystallised on the walls of the ring dyke. As the crystallisation built up, they became gravitationally unstable and thus slumped into the ring dyke, forming the xenolith rich horizons.

Kennedy and Stix (2007) suggest that the Ossippe ring complex (New Hampshire, US) is one of the best examples of a ring complex in the world as it contains a complete ring dyke. The ring complex as a whole is made up of rhyolite and basalt that is encircled by a quartz syenite ring dyke. It is thought that the rocks within this ring dyke show evidence of crystal fractionation, magma replenishment, remelting, rejuvenation, magma mixing, degassing and fragmentation thus presenting a huge variety of magma types. The textural and chemical changes within these rocks are therefore thought to illustrate the history of the ring dyke and it is suggested that it may have been a caldera collapse that caused the ring dyke to be emplaced (Kennedy and Stix, 2007). Kennedy and Stix (2007) suggest that at Cold Brook there is an exposure of multiple rock types that are thought to represent processes that occurred prior to and during caldera formation.

The Sara-Fier complex (Nigeria) is another good example of a ring complex as it is thought that it is made up of five overlapping ring-structures that are aligned in an almost north-south chain. It is suggested that each ring structure is made up of multiple intrusions and that igneous activity had finished at one before the next was formed. It is further suggested that the mechanism of cauldron subsidence is the cause of this complex, with further subsidence creating the successive intrusions (Turner, 1963). The fact that this complex appears to have a constant direction is not thought to have any significance as it is not thought that it can be related to any major tectonic event and in other locations a variable direction can be found, for example, the overlapping ring centres found in Ardnamurchan, Scotland (Turner, 1963).

Another good example of an area which contains several ring dyke complexes is the Blake River Group Mega Caldera Complex (BRMCC), located in Canada, which contains several complexes including the Montsabrais volcanic complex (MVC); the Renault volcanic complex (RVC); and the Jevis South volcanic complex (JSVC). The ring dykes within these complexes vary in diameter from 2km to 12km and are considered to be the remnants of summit calderas (Mueller et al. 2012).

In New Zealand there is a ring complex thought to be of Cretaceous age known as the Blue Mountain Complex. The complex consists of gabbro and lamprophyre ring dykes as well as a marginal alkali gabbro ring dyke; and the complex as a whole covers an area of 1.5km^2. It is suggested that this complex formed due to subsidence of a central block allowing the injection of magma (Grapes, 1975).

2.2.1 Ring dykes within the BIPIP

Within the BIPIP specifically there are several igneous complexes that specifically include a ring dyke, such as the Locahaber Ring Dyke Complex, the Mullach Sgar Complex and the Loch Ba ring dyke (Mull), all of which are located in Scotland, whilst Slieve Gullion provides the best example of a ring dyke on the NE Ireland side of the BIPIP.

2.2.2 Future ring dyke locations

In terms of modern active ring faulting and potential ring dyke emplacement, Mammoth Mountain (California) and Bardarbunga volcano (Iceland) provide suitable tectonic conditions. Prejean et al (2003) study of the Mammoth Mountain involved several computer programs that enabled the modelling of seismic data. Their results suggest that beneath Mammoth Mountain there is an outward dipping ring of seismicity which they suggest to be a ring associated with a normal fault. They further suggest that this ring structure provides a pathway for degassing of magma, which could therefore be thought to further suggest a potential pathway for future ring dyke intrusion. Prejean et al (2003) also suggest that other locations have the outward dipping rings of seismicity, including the Rabaul caldera (Papua New Guinea), Mount Pinatubo caldera (Philippines) and Bardarbunga volcano in Iceland (references therein).

Einarsson et al (1997) also provide data on the seismic events at Bardarbunga volcano (Iceland) as well as suggesting that mapping of the subglacial topography using radio echo sounding has hinted at a large circular structure. The seismicity data presented by Einarsson et al (1997) shows similarities to that of Prejean et al (2003) as the data appears to plot in a circular pattern around the volcano, as well as migrating from one edge of the structure to the other.

2.3 Ring dyke emplacement models

Most models for the emplacement or ring dykes/ring complexes are based on the work of Anderson 1936; cited in Stevenson et al. 2008; Bailey et al 1924; cited in Stevenson et al. 2008 and Richey 1928 and 1932; cited in Stevenson et al. 2008. These researchers are thought to have based their works on the observations of Clough et al 1909; cited in Stevenson et al. 2008 who studied the rocks of the Glen Coe caldera, along with their own observations from various complexes within the BIPIP. In these models it is proposed that subsidence of a central block into a magma chamber along an outward dipping ring fault and subsequent infill of the fault (magma flows up the fracture) that produces ring dykes (Stevenson et al. 2008), shown in Figure 4. Marshall and Sparks (1984) also suggest an emplacement model of subsidence of a central block for their study on net veined and mixed magma ring dykes. They suggest that when the central block subsides it intrudes into an underlying chamber,

causing magma to rise. If this magma mixes with others and if pressure is reduced, gas exsolution can occur and they suggest that this gas expansion may be explosive at shallow depths and would therefore explain veining and brecciation of rocks. They further suggest that if the subsiding block is falling into a compositionally zoned magma chamber, mixing will occur and therefore magmas with a wide range of density may be emplaced in the ring fracture, as can be seen on both Ardnamurchan and St Kilda where a wide range of magmas have intruded the same ring fracture within a short time period. Marshall and Sparks (1984) also suggest three mechanisms that may trigger an intrusive event, which they suggest may or may not lead to an eruption. Firstly they suggest that an influx of new magma into the chamber can increase the pressure to a value that the country rock cannot resist; secondly volatiles are released that also cause overpressure; and lastly subsidence of a central block drives magma into the ring fracture. They conclude that they favour the new magma mechanism as they suggest that nearly all active central volcanic systems show evidence of new magma prior to eruption.

The diagram originally presented here cannot be made freely available via LJMU Digital Collections because of copyright. The diagram was sourced at Stevenson, C.T.E., O'Driscoll, B., Holohan, E.P., Couchman, R., Reavy, R.J., Andrews, G.D.M. (2008) The structure, fabric and AMS of the Slieve Gullion ring-complex, Northern Ireland: testing the ring dyke emplacement model. *Geological Society Special Publications.* 302. 159-184.

Figure 4: Models of ring dyke emplacement, from Stevenson et al. (2008).

Lefrance and John (2001) also seem to agree with a subsidence model as they suggest a cyclical process where pressure builds in the magma chamber leading to fracturing of the country rock which is then subsequently infilled by magma. Pressure then decreases in the magma chamber causing subsidence of the 'roof' along the outward dipping ring fracture. These fractures are again subsequently infilled during the next subsidence event, thus forming the ring dyke structure.

Tuner (1963) also suggests that cauldron subsidence is an adequate model for ring dyke development; however, Tuner (1963) questions Anderson's (1936) idea that this process causes an outward dip. Billings (1945; Turner, 1963) studied ring dykes in New Hampshire and suggested that they actually had vertical contacts and thus upwards dips. Reynolds 1956; cited in Turner, 1963 also disputes that

the process produces outward dips as their research of the Glen Coe ring fault suggests that it has an upward dip that may have once been inward dipping but has undergone marginal tilting. Reynolds 1956; cited in Turner, 1963 also studied the Ossipee Mountains (New Hampshire, US) and suggests that even those ring dykes often have inward dips. Research into Icelandic ring faults suggests that they dip near vertically or steeply inwards and thus it could be thought that a ring dyke occupying this fault would also dip near vertically or steeply inwards (Gudmundsson, 2007). According to the paper presented by Geyer and Marti (2014) the dip of a ring dyke/fault is determined by the mechanical properties between the layers of the host rock therefore, different sections of the ring dyke/fault may show differing dip orientations (outward, inward or vertical). A schematic of this variable dip orientation is shown in Figure 5.

The diagram originally presented here cannot be made freely available via LJMU Digital Collections because of copyright. The diagram was sourced at Geyer, A., Marti, J. (2014) A short review of our current understanding of the development of ring faults during collapse caldera formation.

Figure 5: Sketch of a collapse caldera from Geyer and Marti (2014).

However, some publications suggest that the various dip orientations are indicative of different emplacement styles. Stevenson et al. (2008) suggest that an outward dipping fabric represents a laccolitihic style emplacement (based on their study of the Mourne granite pluton); while O'Driscoll et al. (2006; cited in Stevenson et al. 2008) suggests that an inward dip represents a lopolithic style emplacement (based on their study of Ardnamurchan). Geoffrey et al. (1997; cited in Stevenson et al. 2008), studied the Isle of Skye igneous centre and found that the dip varies from gently to steeply outwards as it approaches the outer wall, and they thus interpreted this as a 'post injection magmatic fabric' which they suggest to be indicative of upward magma flow.

In order to obtain a clear understanding of how collapse calderas form, Geyer and Marti (2014) investigated analogue and numerical models looking at collapse caldera formation. They suggest that there are two main trigger mechanisms that can result in caldera collapse; overpressure within the magma chamber or under-pressure within the chamber. However, they further suggest that there are

several arguments against both of these models. Geyer and Marti (2014) also suggest that caldera collapses consist of a set of ring faults, which may form in one of two ways; it may start at the surface and propagate down until it reaches magma/another structure, or it may start at the magma chamber and propagate up until it reaches the surface. They define ring faults (also called concentric faults) as structures through which rock subsidence takes place during a caldera forming episode, and suggest that these ring faults can be described as either dip-slip (normal or reverse) faults or if there is magma flowing through them (dyke emplacement) mixed-mode propagating structures.

Geyer and Marti (2014) overall suggest that analogue and numerical models are complementary tools in the study of collapse calderas, however when compared against each other they can often provide significantly differing results which may complicate favouring one method over another.

As ring dykes form in ring faults it could be thought that all ring faults will produce a ring dyke however this is not the case. Geyer and Marti (2014) suggest that magma transport may not occur along a ring fault due to several reasons. The first of these being that after the initial subsidence of the central block, the ring fault itself will close and therefore magma will not be able to travel along the fault. However, during the initial subsidence, it is possible that magma transport will occur. The second reason that magma transport may not occur is that the faults themselves may not actually reach the magma chamber. This may be due to the physical location of the fault or due to the magma source being depleted.

3. Slieve Gullion Ring Complex

The Slieve Gullion ring complex together with the igneous centres at Carlingford and the Mourne Mountains, and the Antrim lavas form the northeast Ireland section of the British and Irish Palaeogene Igneous Province (BIPIP) (Troll et al. 2005). These features are considered to represent the major surface exposures of Palaeogene subvolcanic activity in northeast Ireland (Gamble, 1979). The central complexes at Slieve Gullion, the Mourne Mountains and Carlingford lie south of the projected extension of the Southern Uplands Fault, close to the extension of the Iapetus suture, and the Slieve Gullion complex intruded into the Caledonian Newry granodiorite and the Palaeozoic metasediments of the Longford-Down terrane (Gamble et al. 1999). The Slieve Gullion complex is located west of the Mourne Mountains and northwest of Carlingford, in County Armagh and on the border of County Louth. The ring complex is made up of a ring dyke that forms a ring of hills (200-300m high) that surround a younger central sheeted complex (Emeleus et al. 2012). The ring dyke is approximately 12-14km in diameter and consists of two principal lithologies; porphyritic rhyolite and porphyritic microgranite (Troll et al. 2005). It is thought that the large mafic intrusion (~10km thick) beneath the intrusive centre at Carlingford was the feeder for the activity at Carlingford, as well as at Slieve Gullion (Meade et al. 2014). Meade et al. (2014) therefore suggest that this intrusion signifies that there was a large heat source available within the upper crust at this time.

Gamble et al. (1999) investigated the ages for various complexes within the BIPIP, including Slieve Gullion, using U-Pb SHRIMP techniques. Using this technique, they obtained an average age of 56.5±1.3 for the Slieve Gullion complex which shows close agreement with published Rb-Sr data (Meighan, 1988) which provided ages of 57.6±1.0 and 58.5±2.3. Gamble et al. (1999) data provides a range of 13 dates from the Slieve Gullion complex ranging from 55.4 to 62Ma. They therefore place activity at the Slieve Gullion complex in phase 2 of Saunders et al. (1997) timeframe, around 58-55Ma. They suggest that this 3 Ma period is consistent with measurements from the basalts of Mull and Antrim. Current research by Fiona Meade et al. (pers comm), using ^{40}Ar/^{39}Ar, provides new dates for the Slieve Gullion Ring complex that range between 60-62Ma.

Figure 6: Map showing the different lithologies found in the Slieve Gullion ring dyke complex. (Emeleus et al. 2012).

3.1 Lithologies of the Slieve Gullion Ring Complex

According to Stevenson et al. (2008) the Slieve Gullion ring complex is made up of breccias, agglomerates, porphyritic felsite, porphyritic granophyre and cataclasite. The terms porphyritic felsite and porphyritic granophyre are thought to be incompatible with current igneous rock nomenclature and therefore in accordance with the British Geological Survey's classification scheme they are now known as porphyritic rhyolite and porphyritic granite (microgranite) respectively. Richey and Thomas (1932) suggested that the ring complex is composed of the following rocks: 1) Basalt and trachyte lavas which they presume belong to the Antrim group; 2) Volcanic vents of Forkill. These are considered to be filled with volcanic agglomerate and are considered to be explosion breccias that resulted from the degassing of rising magma and are now called the Forkill Breccias; 3) Porphyritic rhyolite. This is suggested to occur as plugs and sheet like bodies; 4) The Breccias of Camlough (now termed the Camlough Breccias). These are considered to be mainly crush breccias; 5) And porphyritic granite which forms a dyke-like body around 270° of the ring (Emeleus et al. 2012). Figure 6 shows the lithologies location as suggested by Emeleus et al. (2012).

The bedrock that this complex intruded into is comprised of Silurian metasediments and the Newry Granodiorite. Stevenson et al. (2008) classified the metasediments as predominately semi-pelites while Troll et al. (2005) classify them as coarse sandstones and shales. The Newry Ganodiorite is approximately 400 Ma (Caledonian) and Gamble (1982) suggests that it has been metamorphosed and partially melted by the combined heat of the Tertiary intrusions.

The Silurian metasediments are made up of coarse sandstones and shales (Troll et al. 2005). Troll et al. (2005) also suggest that these rocks are finer-grained in the southwest than in the north. Stevenson et al. (2008) further suggest that the metasediments are predominantly semi-pelites.

The ring dyke itself is thought to be made up of the porphyritic rhyolite and the porphyritic granite. The rhyolite is Si-enriched on the outer margins of the ring dyke and grades to a less Si-enriched rhyolite towards the inside of the intrusion. The granite however has a higher Si concentration in the centre of the intrusion which grades outwards to lower Si concentrations and this change in concentration is thought to represent the youngest rocks of the intrusion (Troll et al. 2005). McDonnell et al. (2004) used whole rock major and trace element data to suggest that the high-Si rocks form a distinct group, as do the low-Si rocks and that they both formed contemporaneously. They further suggest that these groups originated from the same parent magma rather than being separate igneous events as they suggest that the magma chamber that these magmas originated from was concentrically zoned.

It is thought that the porphyritic rhyolite member of this ring is in two bodies: an inner felsite, that is the more laterally extensive body, and an outer felsite that is laterally more restricted. For the study undertaken by Stevenson et al. (2008) the inner felsite was the main focus. Within this study they noted the presence of lenticular, millimetre to centimetre scale structures which had previously been interpreted as flow banding, however, Stevenson et al. (2008) agree with Bell and Emeleus (1988) that they are actually fiamme structures.

The Camlough breccias are thought to have developed in association with the porphyritic granite member and are thought to be crush breccias and therefore formed in country rock outside the ring dyke and in the outer parts of the porphyritic granite ring dyke (Bell and Emeleus, 1988). Emeleus et al. (2012), describe the Camlough breccias as a zone of intensely veined, deformed and shattered rocks that developed along the outer margin of the ring dyke. They suggest that Camlough-type brecciation shatters and veins the porphyritic microgranite within the ring complex as well as the country rock (Caledonian Newry granodiorite), whereas the metasediments, the porphyritic rhyolite and the Forkill breccias are much less affected.

The Forkill breccias on the other hand, are thought to be associated with the porphyritic rhyolite as they are both restricted to the southwest section of the ring dyke, although the breccias are considered to predate the rhyolite as they lack fragments of the rhyolite but do contain veins of the rhyolite (Stevenson et al. 2008). The breccias are made up of fragments of different country rocks (gabbro, Newry granodiorite, basalt, and metasediments) within a matrix made by pulverised granodiorite, Emeleus et al. (2012). Stevenson et al. (2008) suggest that these breccias formed in situ

due to gas explosions, however, Emeleus et al. (2012) suggest that while one rock type may dominate an outcrop of these breccias, others are normally present which is thought to indicate that they did not form purely due to in situ shattering.

While some authors briefly mention *basalts* within the ring dyke complex or the surrounding area they are not generally discussed in great detail. Richey (1932) suggests that there are remnants of basalt within the Slieve Gullion and Carlingford areas, which they assume belong to the plateau group of the Inner Hebrides and Antrim, and are therefore formed earlier than the Slieve Gullion ring dyke rocks. However, they also suggest that basalt can be found in connection with the Forkill vents (Forkill Breccias). They further suggest that the basalt has a lava origin due to its association with trachyte outcrops. Emeleus et al. (2012) also suggests that the basalt is closely associated with the Forkill breccias, and they also presume that it originally derived from the Palaeogene Antrim lava group. Gamble et al. (1999) also suggest a link between the basalts and the vent breccias (Forkill breccias) however they do not suggest a definite link to the Antrim lavas. They do however suggest that the basalt represents the existence of surface volcanism in the Slieve Gullion area. Both Emeleus et al. (2012) and Gamble et al. (1999) present geological maps within their papers that show the location of various outcrops of the basalts, however the newer paper by Emeleus et al. (2012) suggests that there is less basalt than originally thought by Gamble et al. (1999).

Anglesey Mountain is made up of microgranite which is thought to have intruded the complex after the ring dyke as Stevenson et al. (2008) place it last in their sequence of events.

Patterson (1953) suggests that the porphyritic microgranite and the porphyritic rhyolite have chemical similarities to the Mourne granites, while the porphyritic microgranite also shows similarities to granophyre (microgranite) found in the Carlingford complex. They further suggest that there are chemical similarities (minor elements) between the Slieve Gullion rocks and rocks found in the Antrim lava plateau.

The study undertaken by Troll et al. (2005) investigated Sr and Nd isotope ratios of several rocks from the Slieve Gullion complex. They obtained results for: a Palaeogene basalt dyke ($^{87}Sr/^{86}Sr$: 0.705948±18 and $^{143}Nd/^{144}Nd$: 0.512799±22); the lower Palaeozoic sedimentary country rock ($^{87}Sr/^{86}Sr$:0.722829±20 and $^{143}Nd/^{144}Nd$: 0.512134±7); the Newry granodiorite ($^{87}Sr/^{86}Sr$:0.708136 and $^{143}Nd/^{144}Nd$: 0.512328); and the ring dyke rocks ($^{87}Sr/^{86}Sr$:0.707673 to 0.713593 and $^{143}Nd/^{144}Nd$: 0.512384 to 0.512455). Troll et al. (2005) suggest that their results represent two stages of contamination involving the presence of Longford-Down metasediments and the Newry granodiorite. They propose a model that involves fractionating magmas being contaminated by local sedimentary rocks which produces the rhyolite magmas. This magma then experiences additional contamination

from the Newry Granodiorite. This could be thought to be supported by McDonnell et al. (2004) who suggest that certain trends seen in the trace elements Pb and Zr may be explained through open system fractionation, and subsequent contamination when the Longford-Down metasediments and/or the Newry Granodiorite were encompassed.

Several authors have undertaken specific petrographic/geochemical studies of the Slieve Gullion complex. Emeleus (1961-1963) investigated the porphyritic rhyolite and suggested that it was chemically similar to other siliceous rocks within the BIPIP, such as those found on the Isle of Skye. Gamble (1982) used electron microprobe analysis to study the chemical mineralogy of a granodiorite from the slopes of Slieve Gullion and two hybrid rocks from contacts between the granodiorite and the Palaeogene intrusion (ring dyke). Gamble (1982) concluded that the Newry granodiorite was metamorphosed and partially melted although the composition remained mostly unchanged. O'Connor's (1988) study involved the investigation of strontium isotopes from several of the Irish Igneous centres. From the results that they obtain for the Slieve Gullion complex they suggest that the earliest rocks are represented by the higher $^{87}Sr/^{86}Sr$ ratio (0.7141±0.0005) while the latest are represented by lower ratios (0.708 to 0.709). They continue to suggest that this trend in isotopic ratios represents substantial crustal contribution for the magmas that were formed first. Magmas that were produced after this have lower ratios which they suggest reflects dilution of the crustal component.

Troll et al. (2008) and Emeleus et al. (2012) both suggest that within the Slieve Gullion ring dyke complex, tuffisites can be found, in the porphyritic microgranite and the marginal porphyritic rhyolite. According to Kolzenburg et al. (2012) it was Cloos (1941) who first described tuffisites. Cloos (1941) described the tuffisites as a host rock that had been infiltrated by "tuff" along its cracks and crevices. Garfunkel and Katz, (1967) extend Cloos, (1941) definition by suggesting that tuffisites can be 'any mixture of fragmented and conminuted country rock with or without primary magmatic material'. They therefore suggest that their use of the term tuffisite refers to many types of fragmented and brecciated rocks that have formed due to gas streaming by fractures which is connected to magmatic activity. Berlo et al. (2013) define tuffisite veins as glass filled fractures that form during degassing of a magma conduit. They further suggest that these veins form channels that allow gases to escape. Within the research undertaken by Troll et al. (2008), in the Slieve Gullion area, tuffisites are defined as a rock resulting from fracturing of magma that has material that has been transported by a fluid phase.

3.2 Emplacement models of the Slieve Gullion Ring Complex

According to Emeleus et al. (2012) it was Richey, (1928) who provided the original ring dyke emplacement model. In Richey's (1928) model, it was suggested that a central block subsides along an outward dipping ring-fault, opening up a ring fracture into which magma is then injected thus forming the ring dyke.

3.2.1 Is it a ring dyke?

Stevenson et al. (2008), however, questioned this model with regards to the Slieve Gullion ring complex and used a combination of field observations, detailed structural measurements and anisotropy of magnetic susceptibility measurements (AMS) to provide an alternative model. They suggested that while ring-faulting may have played a role in the development of the complex, there was a lack of exposed contacts and little fabric evidence to support Richey's model of magma intrusion along a steep, outward dipping ring-fault. Stevenson et al. (2008) suggest that the porphyritic rhyolite and the porphyritic microgranite were emplaced as separate events in significantly different emplacement modes due to the differing internal structures and contact relationships, neither of which can be explained through the traditional ring dyke model. They therefore suggested that the porphyritic rhyolite represented the down-faulted vestige of a moderately welded ignimbrite sheet; while the porphyritic microgranite represented the lower part of an originally gently outward dipping intrusive sheet (laccolithic intrusion). The emplacement sequence suggested by Stevenson et al. (2008) in place of the ring dyke model involves five stages. The first stage is initial eruption with incipient ring-faulting and subsidence followed by stage two: collapse. This involved more subsidence along with ignimbrite eruption, ring-fault development and caldera collapse. The third stage involved initial resurgence and emplacement of the porphyritic microgranite as a sheet close to the base of the subsided ignimbrite. This led on to the main phase of resurgence which involved emplacement of the central complex which partly intruded the porphyritic granite sheet, resulting in doming. The last phase of the suggested sequence is the emplacement of Anglesey Mountain (a late microgranite body). This sequence of proposed events is shown in Figure 7.

3.2.2 Traditional ring dyke view

Troll et al. (2008) use their investigation of a motorway outcrop at Ravensdale (Co. Louth) to suggest that they do not support the model put forward by Stevenson et al. (2008). In their investigation, Troll et al. (2008) record a contact between the Silurian metasediments and the porphyritic microgranite that is locally intensely crushed. They suggest that this crushed zone extends for more than 2 metres into both lithologies which indicates the presence of a major fault. They also suggest that this crushing is similar, although more severe, to other localities within the Slieve Gullion complex and that it also

shows similarities to classic caldera complexes such as Glen Coe. Troll et al. (2008) also report that the internal textures in the porphyritic microgranite shows similarities to silicic feeder dykes found in Iceland, which they suggest helps support the idea of upward-directed caldera-related magma transport within the Slieve Gullion ring complex. They therefore also support the more traditional view of a ring dyke as they believe that their field data does resemble the model put forward by Richey and Thomas (1932). They do however acknowledge that the emplacement mechanism may not be exactly as envisaged by Richey and Thomas (1932).

Emeleus et al. (2012) suggest that while new knowledge may provide reasoning for a reappraisal of the 'traditional' ring dyke model they have reservations regarding the model suggested by Stevenson et al. (2008). Firstly, they suggest that while Stevenson et al. (2008) suggest that there is a lack of contacts visible in the Slieve Gullion region, there are in fact some examples of sharp contacts in the area and several authors have documented these. Secondly, Stevenson et al. (2008) suggest that there is a lack of steep shear fabrics and that there is a flat lying fabric (from the AMS study) which they believe represents a horizontally emplaced sheet, however Emeleus et al. (2012) suggest that ring dyke emplacement can result in a chaotic particle movement which suggests that the fabric may not represent the direction of flow. Emeleus et al. (2012) further suggest that the absence of a steep fabric does not disprove the ring dyke model as AMS data can be difficult to interpret. It is generally thought that AMS records the final movements of a liquid before it solidifies. As magma emplacement may include a combination of magma flow, compaction, crystal growth and other processes, any AMS data obtained may be affected as it is suggested that the data may not represent purely magma transport.

Another point that Emeleus et al. (2012) question is the suggestion that the porphyritic rhyolite may be an ignimbrite flow and that the Forkill breccias are the result of an avalanche deposit. They suggest that if this is the case, the Forkill breccias, which overlie the rhyolite, must therefore post-date the rhyolite and it would be expected that the breccias would include fragments of the rhyolite. However, rhyolite is not common in the Forkill breccias and the few examples that do occur are restricted to the margins of the ring-complex. Emeleus et al. (2012) suggest that the exposed contacts and the occurrences of dykes and veins of rhyolite overall implies an intrusive origin for the rhyolite.

From field, petrographic and geochemical evidence from the rhyolite and microgranite members of the Slieve Gullion complex, Emeleus et al. (2012) suggest that this complex can be defined as a ring dyke. They also suggest a series of events that resulted in this complex, beginning with a large body of mafic magma which intruded into the southwestern granodiorite pluton of the Newry Igneous Complex. This generated silicic magma through fractionation of basaltic magma and melting and partial melting of Newry granodiorite and the Silurian metasediments. The ring complex was formed

when a ring-fault occurred above this magma system, causing caldera subsidence. This was accompanied by shattering of the faulted rocks which formed the Camlough breccias. Further release of gases from the magma is thought to have produced the Forkill breccias. Emeleus et al. (2012), also suggest that the porphyritic microgranite emplacement overlapped with the emplacement of the porphyritic rhyolite, and was further accompanied by movement of the ring-fault, continuing the release of gases and tuffisite injection. Emeleus et al. (2012) lastly suggest that the Slieve Gullion complex does not need reinterpreting and favour the caldera related ring fault model, however it may be possible that certain aspects could be viewed differently due to new knowledge derived from exposed ring-centres, active caldera volcanoes and experimental and numerical simulations.

Figure 7: Diagram showing the proposed emplacement model for the Slieve Gullion complex from Stevenson et al. (2008).

3.3 Fault Structures of the BIPIP

Within the Slieve Gullion ring dyke complex there are several major fault structures. Gamble et al. (1992) produced a diagram (see Figure 8) highlighting the location of the Slieve Gullion (and other Palaeogene igneous complexes) in relation to the NE-SW faults that extend from Scotland. From this diagram it can be seen that the Slieve Gullion ring dyke complex lies south of the Southern Uplands Fault (SUF) and north of the Iapetus Suture (IS). It can also be seen that there are three faults perpendicular to the SUF and IS, that cut through the Slieve Gullion ring dyke complex in a NW-SE direction, one of these being the Newry Fault.

The map originally presented here cannot be made freely available via LJMU Digital Collections because of copyright. The map was sourced at Gamble, J.A., Meighan, I.G., McCormick, A.G. (1992) The petrogenesis of Paleogene microgranites and granophyres from the Slieve Gullion Central Complex, NE Ireland. *Journal of the Geological Society.* 149. 93-106.

Figure 8: Map showing the location of the Slieve Gullion ring dyke complex (and others) with the location of associated major faults (Gamble et al. 1992).

Emeleus et al. (2012) also present a diagram showing a more detailed map of the Slieve Gullion ring dyke complex which shows the location of several smaller faults. In the north-western section of the ring dyke complex, there are several faults that strike NNW-SSE. There are also two larger faults that cut across nearly the whole of the complex that strike in the same direction. In the south-western and north-eastern sections of the ring dyke, there are multiple NE-SW trending faults, with the south-western section showing some small NW-SE trending faults also.

3.4 Field methods and Study Sites

During the field work for this study a combination of detailed field observations, mapping, rock sample collection and structural measurements were used in selected field locations around the ring dyke

complex. The sites used for this study are shown in Figure 9 and a list of those samples that were sent for geochemical analysis and thin section production is shown in Table 2.

The map originally presented here cannot be made freely available via LJMU Digital Collections because of copyright. The map was sourced at Emeleus, C.H.,Troll, V.R., Chew, D.M., Meade, F.C. (2012) Lateral versus vertical emplacement in shallow-level intrusions? The Slieve Gullion ring-complex revisited. *Journal of the Geological Society.* 169. 157-171.

Figure 9: Location of field sites (green dots) used for this study. Map adapted from Emeleus et al. (2012).

Site Number	Site Name	GPS	Sample Number	Preliminary Rock Identification	Thin Sections	Geochemical Analysis
1	Forkill Quarry	J 005 162	1	Basalt	✓	✓
1	Forkill Quarry		2	Rhyolite	✓	✓
1	Forkill Quarry		3	Basalt	✓	✓
2	Ballynamadda Road	J 033 149	4	Rhyolite	✗	✓
2	Ballynamadda Road		5	Rhyolite	✓	✓
3	Camlough Quarry	J 039 246	6	Granite	✓	✓
3	Camlough Quarry		7	Sediments	✓	✓
3	Camlough Quarry		8	Sediments	✓	✓
4	Forkill Breccias	J 080 825	9	Breccia	✗	✗
4	Forkill Breccias		10	Breccia	✓	✓
5	Cashel Road 1	J 977 177	11	Granite	✓	✓
5	Cashel Road 1		12	Rhyolite/Granite	✗	✗
6	Cashel Road 2	J 976 182	13	Sediments	✓	✓
7	Cashel Road 3	J 976 181	14	Granite	✓	✓
8	Glassdrumman Pier		15	Granite	✗	✗
9	Croslieve Mountain	J 334 316	16	Rhyolite	✗	✓
10	Tievecrom Road	J 034 148	17		✗	✗
11	Ravensdale Forest		18		✓	✗
1	Forkill Quarry	J 005 162	19	Rhyolite/Granite	✓	✓
1	Forkill Quarry		20	Sediments	✗	✗
1	Forkill Quarry		21	Breccia	✓	✓
12	Outskirts 'basalt'	J 961 187	23	Basalt	✓	✓
13	Forkill House	J 627 148	24	Rhyolite	✓	✓
3	Camlough Quarry	J 039 246	25	Sediments	✗	✗
3	Camlough Quarry		26	Sediments	✓	✓
3	Camlough Quarry		27	Sediments	✗	✓
3	Camlough Quarry		28	Sediments	✗	✗
14	Mullaghbane Golf Course	J 988 179	29	Rhyolite	✓	✓
16	Slieve Gullion Central Complex		30	Gabbro	✗	✓
16	Slieve Gullion Central Complex		31	Granite	✓	✓
15	Dublin Road	J 080 246	32	Granite	✓	✓
15	Dublin Road		33	Granite	✗	✗

Table 2: Sample number and site information with corresponding analysis information (geochemistry and thin sections). Rock identification based on field observations. The number of the samples corresponds to the order in which they were collected. GPS information used the Irish Grid.

4. Geochemical and Petrographic Methods

4.1 Geochemical classification

The geochemical classification of rocks is essential to enable effective communication between petrologists; a specific rock name should convey the same meaning to every petrologist. This can prove difficult as it thought that within igneous rocks alone there are around 800 different rock names in use. The International Union of Geological Sciences Sub-commission on the Systematics of igneous rocks (IUGS) is thought to be a universal standard that everyone is able to use and it involves plotting silica content (SiO_2) against the total alkalis content ($Na_2O + K_2O$) (Best and Christiansen, 2001). However, there are several other geochemical classification systems available.

Raymond (1997) suggests that the sheer number of rock names in the literature is problematic as some names were created for rocks at specific locations or rocks from the same location with differing mineralogies. He also suggests that the basis of a classification scheme can be problematic as different classification schemes use a different basis, i.e. mineralogy, chemistry, texture, geographic location and/or rock associations. Raymond (1997) suggests that classifications that use rock associations (rock suites, series or families) are widely used and are based on mineralogy, texture and chemistry. Texture is a parameter that is thought to be used by most petrologists, as it enables the classification of rocks into two or more categories. Mineralogy is thought to be the second major parameter.

Classification of rocks is also important as the geochemistry of rocks can vary from province to province, volcano to volcano and within a complex, which highlights the difficulties that can be faced when attempting to name a rock (Cox et al. 1979).

The geochemistry of a rock in itself can be a complex issue. Differences in the cooling environment and the rate of cooling can have a huge effect on the nature of a rock as different constituents of the magma will crystallise at different temperatures. The range of minerals that forms during cooling depends on the rate of cooling and the initial temperature of the magma. The composition of a rock can also be effected by the type of melting process that it undergoes, as well as if there is any partial melting. The composition can also be substantially modified on its way to the surface/cooling (Rollinson, 1993).

4.2 What information is needed for geochemical analysis?

To obtain geochemical information several methods can be used: x-ray fluorescence (XRF), neutron activation analysis (INAA and RNAA), inductively coupled plasma emission spectrometry (ICP), atomic absorption spectrophotometry (AAS), mass spectrometry, electron microprobe analysis, and the ion microprobe. To obtain the percentage of major elements, it is thought that XRF and ICP are the most versatile methods. Using XRF means that the sample has to be prepared as a glass bead whereas using

the ICP method means the sample has to be in solution. The ICP method is faster than XRF, however XRF is more precise. To obtain the trace elements several of the above methods can be used. Again XRF and ICP are the most versatile however INAA, RNAA, IDMS and SMSS enable the detection of lower concentrations of elements. To obtain the rare earth elements IDMS is the most precise however ICP and XRF still yield good results (Rollinson, 1993).

4.3 What geochemical data can show

4.3.1 Classifications

Summerfield (1991) suggests that a basic classification of igneous rocks can be made using the mineral and chemical composition and differences in grain size. Igneous rocks can also be classified based on their silica content (SiO_2); acid rocks contain more than 66%, intermediate 52-66%, basic 45-52% and ultrabasic <45%.

Cox et al. (1979) suggest that two of the most important chemical parameters to be used are SiO_2 and the total alkalis (Na_2O and K_2O). The SiO_2 and total alkalis have been plotted against each other, and the names of rocks have been added to the geochemical classification diagram. If this method is used to name a rock then it may be possible to predict the main features of that rock, as the original investigators will have used more than the SiO_2 and total alkalis when deciding on these classifications. There is some debate over the usefulness of this diagram and some suggest a point of disagreement in the use of some terms. For example, the use of the term trachyandesite, in some diagrams plots in the fields of mugearite and benmoreite, whereas Cox et al. (1979) prefer to use the term trachybasalt. They place trachyandesite between trachyte and andesite.

Frost et al. (2001) suggest a classification scheme for granitic rocks that uses chemical data, major element compositions and is flexible enough to accommodate the wide range of compositions found in granitic rocks. They propose a three-tiered scheme. The first tier uses the FeO/(FeO +MgO) ratio of the rocks (this shows information about the differentiation history of the granitic magma). The second tier uses a modified alkali-lime index ($Na_2O + K_2O - CaO$) (this is related to the source of the magma). The third tier is the aluminium saturation index (the micas and minor minerals) which is related to the source of the magma and the conditions of melting.

Frost and Frost (2008) extended this classification scheme to enable its use for feldspathic igneous rocks. To do this they added two additional parameters; the alkalinity index (AI) and the feldspathoid silica-saturation index (FSSI). They suggest that by adding these indices, the original classification can be extended to include alkaline rocks. They do however further suggest that even this improved classification does not work well for basaltic rocks.

De La Roche et al. (1980) characterised igneous rocks using the R_1 and R_2 variables. They suggest that these variables take into account any variation in silica saturation as well as changes in the Fe/(Fe+Mg) ratio and plagioclase compositon (associated with differentiation).

A classification proposed by Pearce et al. (1984) is thought to characterise the tectonic environment of granitic rocks (ocean ridge granites, volcanic arc granites, within plate granites and collisional granites). They proposed that the best graphical representations to distinguish these environments are plots of Nb vs Y, Ta vs Y, Rb vs (Y + Nb) and Rb vs (Y + Ta). They suggest that this method of classification is especially useful if the tectonic setting has not been preserved.

Gillespie and Styles (1999) used the IUGS classification system however they changed some aspects of the system where they believed it to be necessary and they suggest that the resulting scheme is more logical, consistent, systematic and clearly defined. Their scheme is a hierarchical scheme which they suggest enables less skilled scientists to use the lower levels (with less information) while higher levels can be used where more information is available. Their scheme is presented in the form of a flow chart, enabling a scientist to follow the correct path to obtain the correct name of the rock and their classification is based on descriptive attributes (grain size, composition). They do however suggest that this method can result in rock names that are much longer than 'traditional' names.

Classifications can also be made regarding the tectonic environment that the rocks were produced in, such as that created by Ewart (1982) which places rocks into one of four categories based on SiO_2 and K_2O concentrations. These four categories include; alkaline series, high-k calc-alkaline series, calc-alkaline series and low-k series. This can help to provide an age constraint or can give an idea to potential sources of contamination.

4.3.2 Variation diagrams

Generally, chemical compositions of rocks are presented by petrologists in two formats: tables of oxide and/or element concentrations; and graphs where points represent the concentrations of chemical constituents. These graphs (variation diagrams) show trends or patterns in the chemical data (Best and Christiansen, 2001).

The most commonly used types of variation diagrams are Harker diagrams, where an oxide is plotted against SiO_2. It is suggested that trends on these diagrams represent the course of the chemical evolution of magma and are referred to as liquid lines of descent. Specifically for igneous rocks the triangular ARM variation diagram can be used (A = Na_2O, F = FeO + Fe_2O_3, M = MgO) which distinguishes between tholeiitic and calc-alkaline differentiation trends in the sub-alkalic magma series (Wilson, 1989).

4.4 Laboratory methods

Within the laboratory the rock samples were prepared for geochemical analysis and the production of thin sections. This involved firstly cutting each rock sample in half and then cutting one half into a cube. The cube was then sent off to be made into a thin section of rock at the department of Earth Sciences in Durham University, while the offcuts were sent for geochemical analysis at Activation Laboratories Ltd, in Canada. The process of creating the samples to be sent for analysis was not as selective as was necessary, therefore the samples sometimes contained other rock types and weathered crusts.

For the geochemical analysis, the samples were sent to a laboratory in Canada, where they used mass spectrometry to obtain major and minor elements. The laboratory used a combination of lithium metaborate/tetraborate fusion ICP whole rock and trace element ICP/MS to obtain the geochemical data.

To study the textures and internal structures of the igneous rock samples using thin sections or rocks, a polarizing petrographic microscope was used.

5. Results

The different rock units of the Slieve Gullion ring dyke complex are described in order of emplacement from the oldest to the youngest rock unit as follows; the bedrock, which is made up of Silurian metasediments and the Newry Ganodiorite; Basalt unit; the ring dyke itself, which is made up of porphyritic rhyolite and porphyritic microgranite; the Forkill breccias; and the central sheeted unit. Each rock unit will be discussed in terms of field outcrop, hand sample and thin section observations. A general map showing all the study site locations is shown in figure 9.

5.1 Silurian Metasediments

Within this study the Silurian metasediments can be found in both the Forkill Quarry (Site 1) (Figure 10) and the Camlough Quarry (Site 3) (Figure 11). Within the Forkill quarry several examples of folds can be seen within the metasediments as well as clusters of calcite crystals which are associated with fractures. These outcrops also often look extremely crushed. The Forkill quarry also provides a good exposure of the contact between the Silurian metasediments and the porphyritic rhyolite. The metasediments in the Camlough quarry also show intense crushing in certain locations, as well as containing thin veins of granite and occasionally $CaCO_3$. One 'wall' of the metasediments in the Camlough quarry contains less fractures as this is likely the bedding plane, however in this 'wall' examples of tuffisite veins can be found. In the north east corner of the Camlough quarry is the contact between the metasediments and the porphyritic microgranite. This contact shows some metamorphic colour change to the metasediments, in a section that extends for about 15cm. There are also veins of granite running into the metasediments.

As can be seen in the hand samples of the Silurian metasediments (Figures 12 and 13), the samples are very fine grained and show distinct bands (layers) that are mostly black and grey, however in the Camlough quarry there are more occurrences of white bands. In the hand samples from the Camlough quarry the tuffisite veins can be seen, which look to be made up of veins of biotite.

The thin sections from the metasediments samples (Figure 14) show a combination of fine and coarse bands of quartz crystals, which reflects the layering that can be seen in the field.

Figure 10: Contact (red line) between the Silurian metasediments and the porphyritic rhyolite in the Forkill Quarry (Site 1).
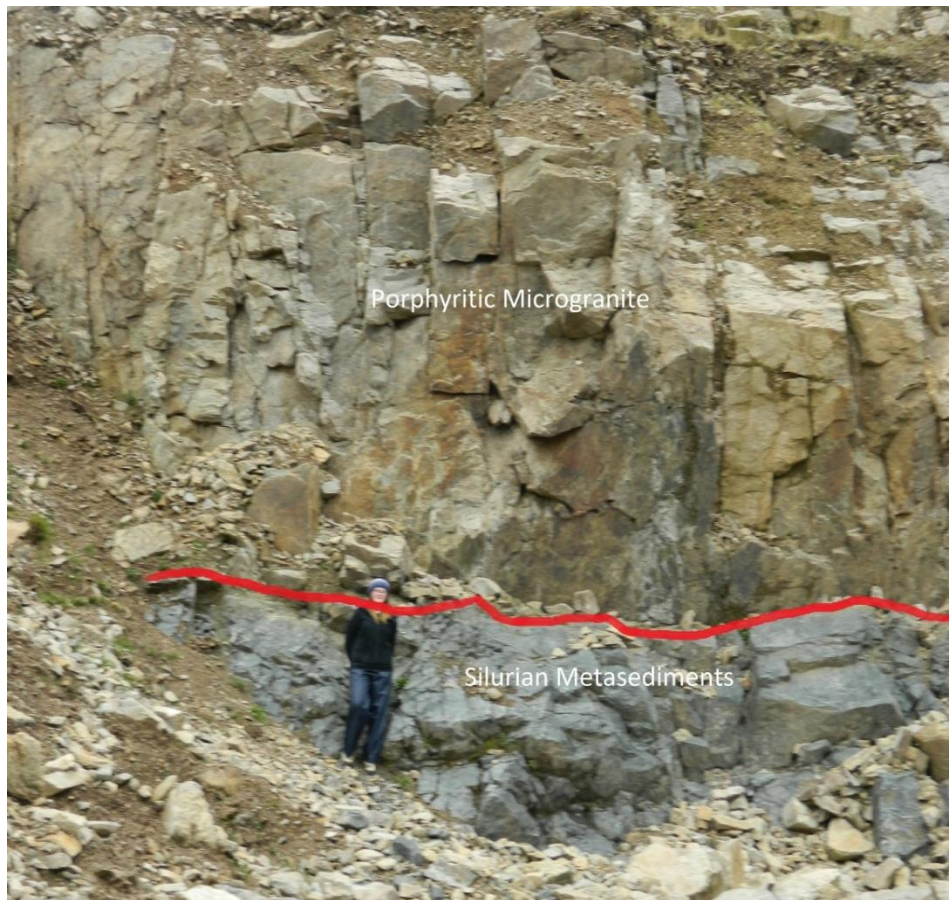
Figure 11: Contact (red line) between the Silurian metasediments and the porphyritic microgranite in the Camlough Quarry (Site 3).
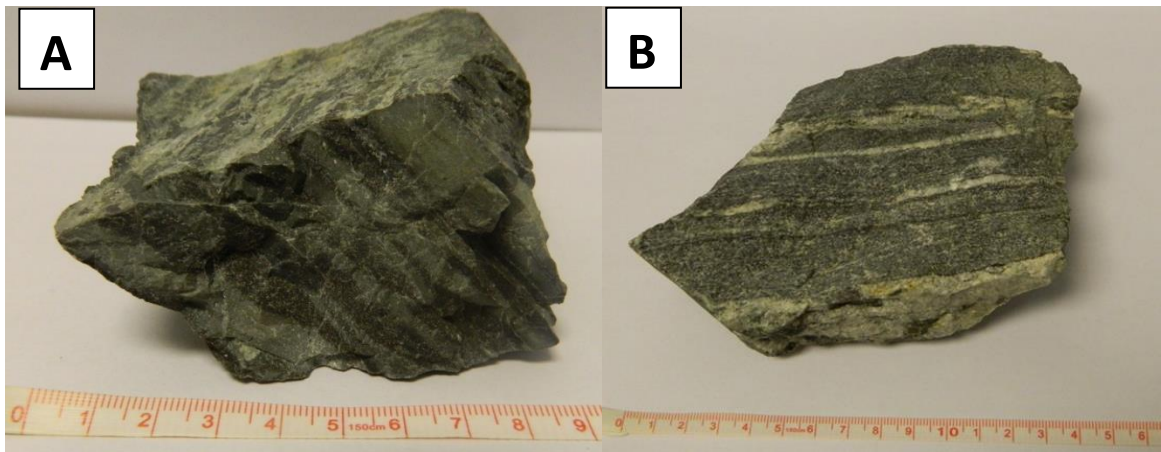
Figure 12: A: Photograph of sample 21 from site 1 (Silurian metasediments). B: Photograph of sample 26 from site 3 (Silurian metasediments).

Figure 13: Photograph of the bands within the Silurian metasediments at site 3, showing the presence of tuffisites (red arrow).
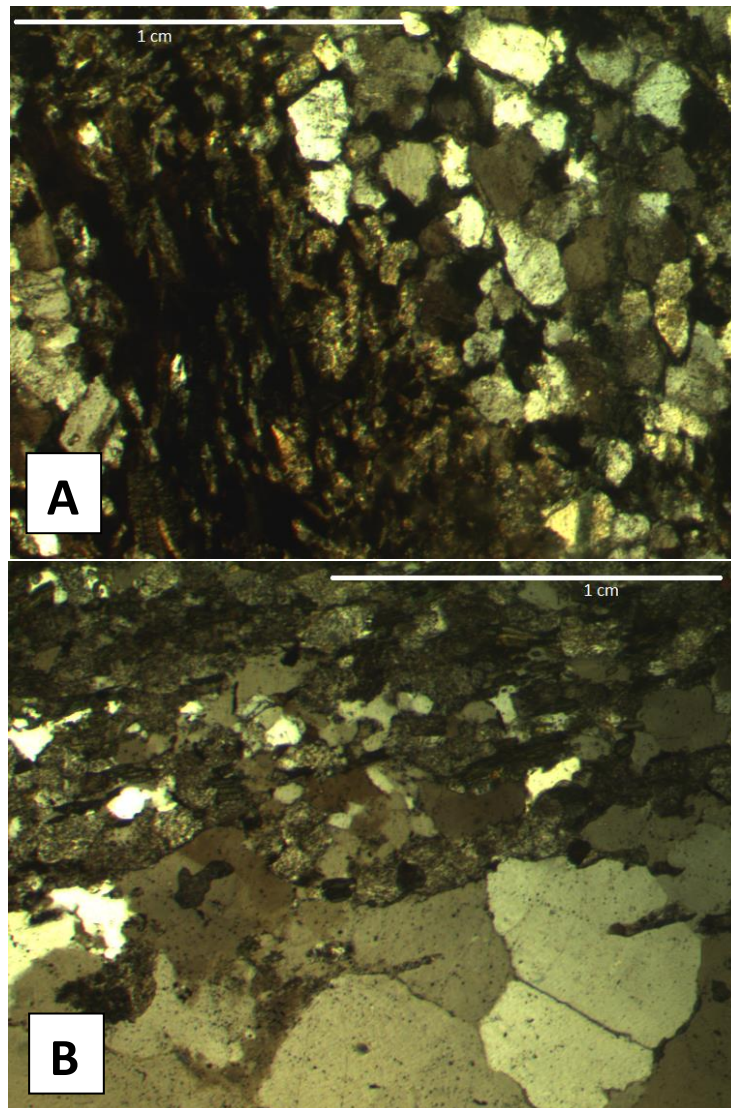
Figure 14: A: Thin section photograph (crossed polars) of sample 8 (site 3), showing the different bands within the Silurian metasediments, made up of quartz crystals. B: Thin section photograph (crossed polars) of sample 26 (site 3), showing the bands within the Silurian metasediments, made up of quartz.

5.2 Newry Granodiorite

Only one site (Site 15) was used within this study to study the Newry granodiorite. This outcrop (Figure 15) is located on Dublin Road, close to Newry City, and is grey in colour with multiple fractures that have two preferred orientations. The hand sample from this site (sample 32) shows a dark coarse grained granite (Figure 16) and the thin section (Figure 17) for this samples shows large crystals of biotite and of plagioclase which shows evidence of hydrothermal alteration.

Figure 15: Outcrop of Newry granite, site 15. Notice the presence of near vertical fractures.

Figure 16: Photograph of sample 32 (site 15), Newry granite.
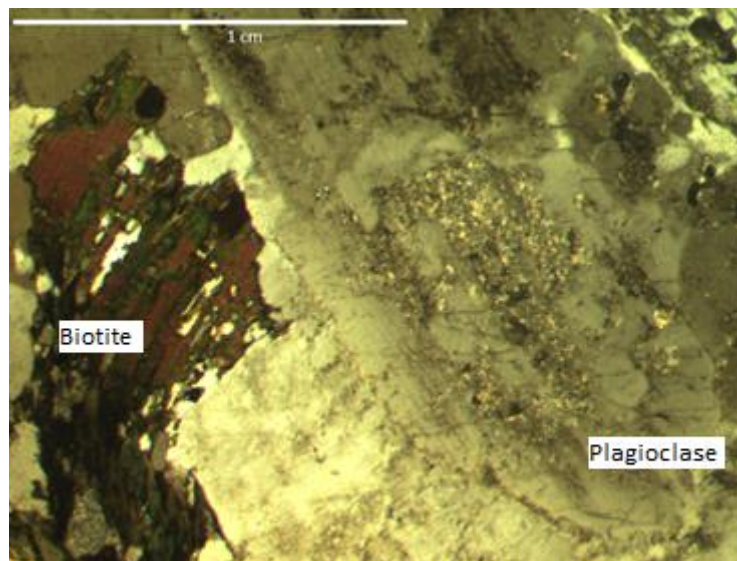
Figure 17: Thin section photograph (crossed polars) of sample 32 (site 15), showing hydrothermal alteration of plagioclase crystals within the Newry granite.

39

5.3 Basalts

The basalt studied here was only found in one site, the Forkill quarry (Site 1), as several rafts within the porphyritic rhyolite (Figure 18). These rafts show some fracturing and veining, however the most notable feature on one of these rafts was the presence of small (<5mm) spherical inclusions (Figure 19) that look to be made up of the same rock.

The hand samples taken from these rafts (samples 1 and 3) show a fine grained rock that is blue/grey in colour with evidence of fine veins of calcite ($CaCO_3$) which is associated with hydrothermal activity (shown in Figure 20).

The thin section from sample 1 (Figure 21) shows a fine matrix with coarse inclusions that are well-rounded. It is suggested here that these are inclusions of gabbro (xenoliths) that the basalt picked up on its way through the magma chamber. The sample 3 thin section also shows these spherical inclusions however they are slightly less coarse than those seen in sample 1.

Figure 18: Rafts of basalt (highlighted in red) within the porphyritic rhyolite at Site 1 (Forkill quarry).

Figure 59: Photograph of spherical inclusions (xenoliths) on a basalt raft at site 1 (Forkill Quarry).

Figure 20: A: Photograph of sample 1 (site 1), basalt. B: Photograph of sample 3 (site 1), basalt showing fine calcium carbonate veins.
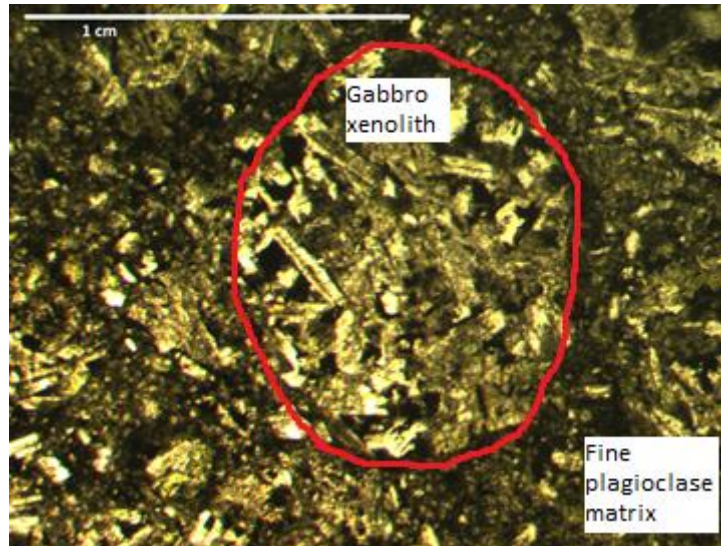
Figure 21: Thin section photograph (plane polars) of sample 1 (site 1), showing coarse rounded inclusions (xenolith of gabbro) highlighted in red, within a fine matrix of basalt (made up of plagioclase).

5.4 Porphyritic Rhyolite

Several sites used in this study contain outcrops of the porphyritic rhyolite (Sites 1, 2, 5, 6, 7, 9, 13 and 14), the most notable of which being the Forkill quarry (Site 1) where the porphyritic rhyolite contains rafts of basalt and inclusions of granite which are thought to be examples of the Forkill breccias. Site 9 (Croslieve Mountain) and site 14 (Mullaghbane golf course, shown in Figure 22) also both contain examples of the fiamme structures found within the complex, with the former site also containing examples of xenoliths of other rock types.

When observing the hand samples it can be seen that they all generally show a fine matrix with larger crystals (Figure 23) that often darker than the matrix or pink in colour (Figure 24). The sample from site 5 seems to have larger 'pink' crystals than previous sites while the sample obtained from the golf course is overall more pale in colour than the other sites, however is still shows similar porphyritic characteristics. Several of the hand samples also show a weathered crust/outer layer and the fiamme structures that can be seen in the outcrop can be seen in the hand sample taken from the golf course (Figure 25).

In general, the thin sections (Figure 26) from the porphyritic rhyolite all show a fine matrix with larger crystals, although there are some examples of alteration of the larger crystals in the form of reaction rims and rings of broken minerals around the crystals, suggesting a xenolith. The sample obtained from the Forkill quarry also shows flow banding that flows around the larger crystals.
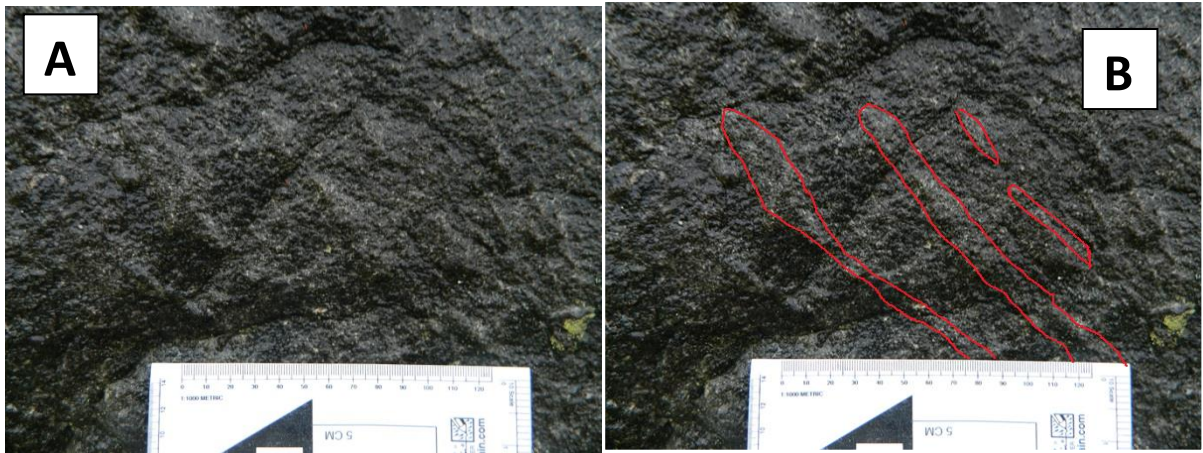
Figure 22: A: Photograph of porphyritic rhyolite at site 14 (Mullaghbane golf course). B: Repeated photograph with fiamme structures highlighted in red.

Figure 23: Photograph of sample 2 (site 1), porphyritic rhyolite.
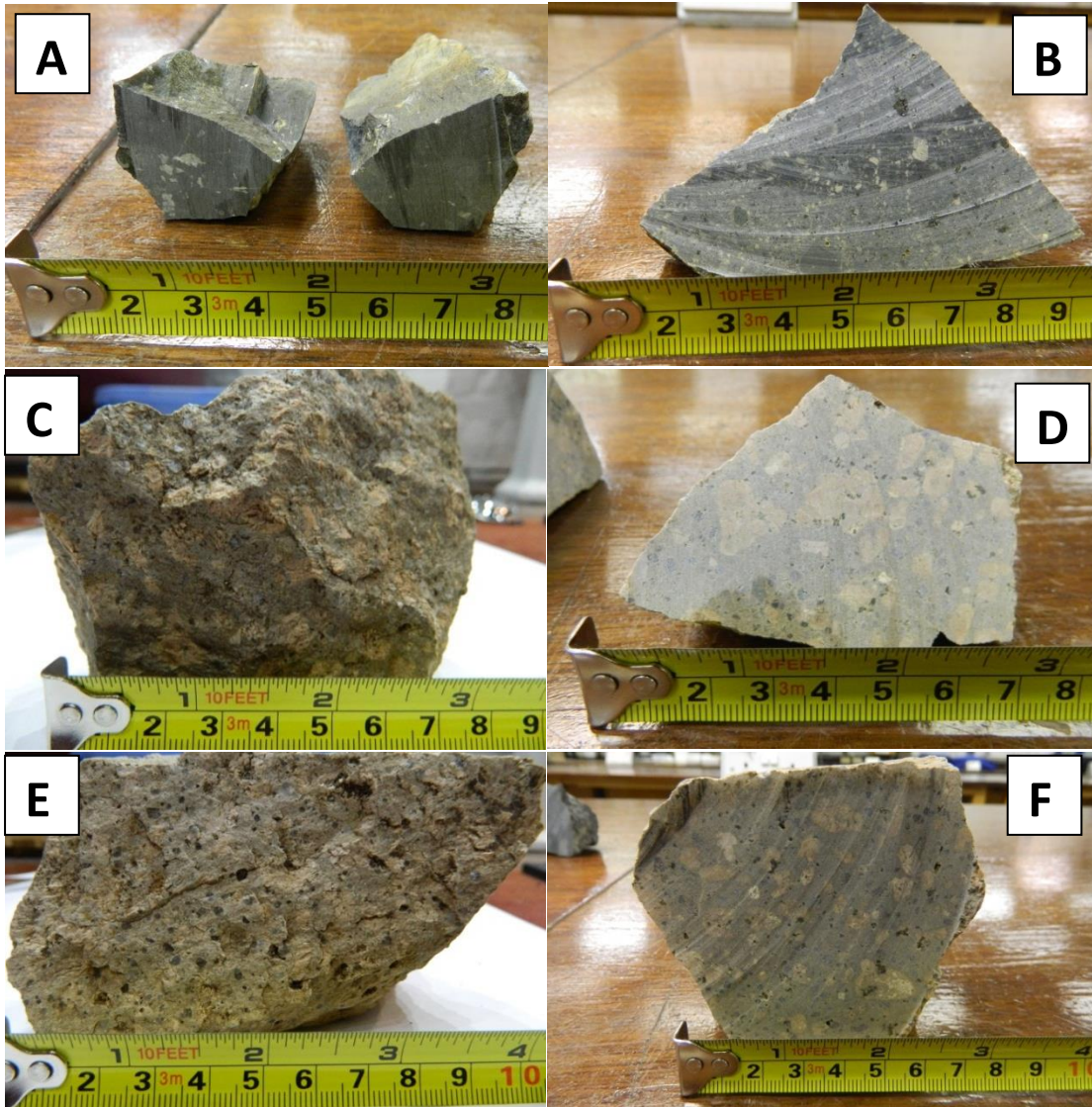
Figure 24: Photographs of porphyritic rhyolite hand samples from different field sites: A: Sample 4, site 2. B: Sample 5, site 2. C: Sample 11, site 5. D: Cut through section of sample 11, site 5. E: Sample 12, site 5. F: Cut through section of sample 12, site 5.

Figure 25: Photograph of sample 29 (site 14), porphyritic rhyolite with fiamme structures (pale parallel lines).
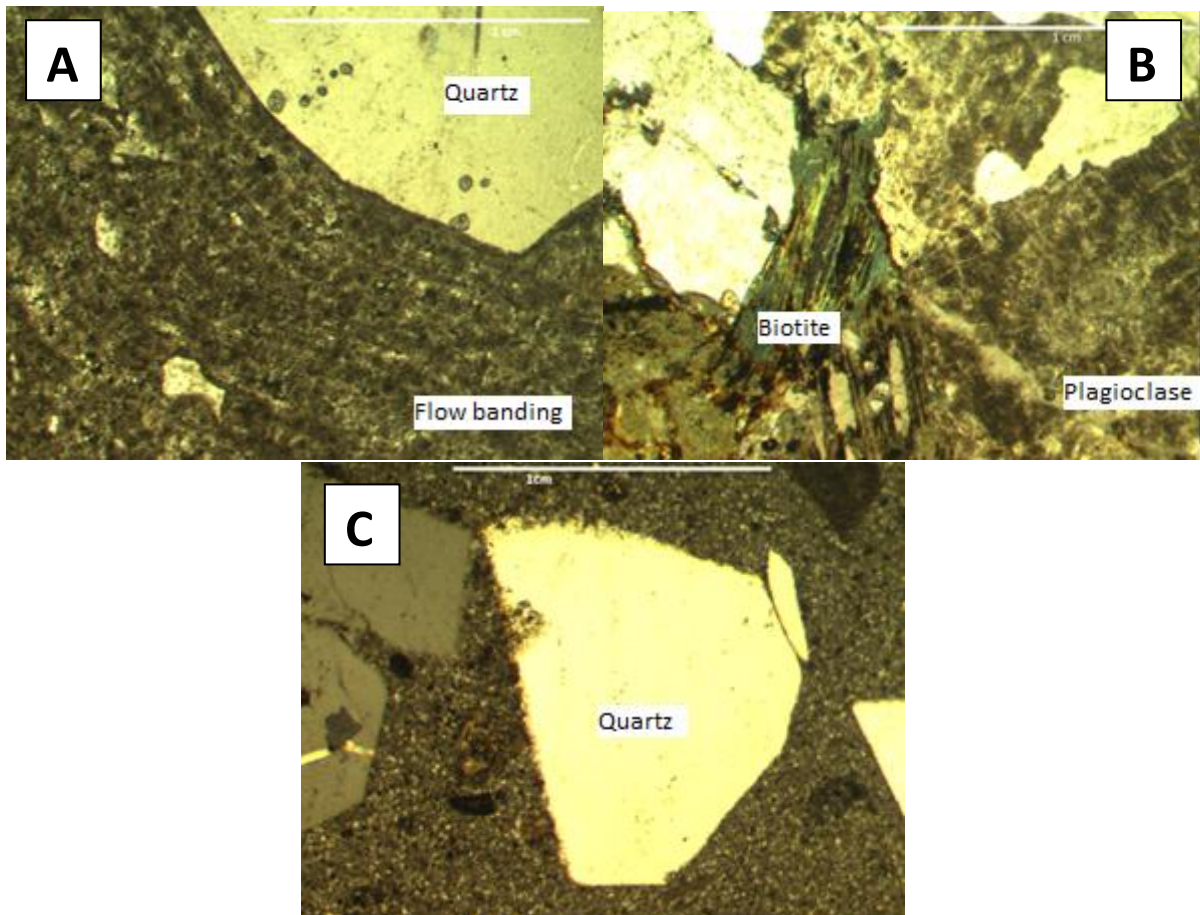
Figure 26: Thin section photographs of the porphyritic rhyolite. A: Sample 2 (site 1) showing flow banding within the fine quartz matrix around a large quartz crystal (crossed polars). B: Sample 14 (Site 7) showing hydrothermal alteration of plagioclase crystals (crossed polars). C: Sample 29 (Site 14) showing a large quartz crystal with reaction rim within a fine quartz matrix (crossed polars).

5.5 Porphyritic Microgranite

The porphyritic microgranite was only studied in the Camlough quarry (Site 3) (Figure 11). Within this quarry the contact between the metasediments and the microgranite is in the north east corner, with the porphyritic microgranite being the top rock unit. The porphyritic microgranite itself is very weathered and extremely fractured, with the fractures showing a preferred orientation. From blocks of the granite that can be found on the quarry floor, it can be seen that this rock contains the tuffisite veins previously mentioned in the Silurian metasediments.

In hand sample (Figure 27) the porphyritic microgranite is very coarse and is mostly grey with black, white and large orthoclase pink crystals, as well as the tuffisites found within this complex.

The thin section for the microgranite (Figure 28) shows a typical granite, with quartz, biotite, plagioclase and orthoclase.
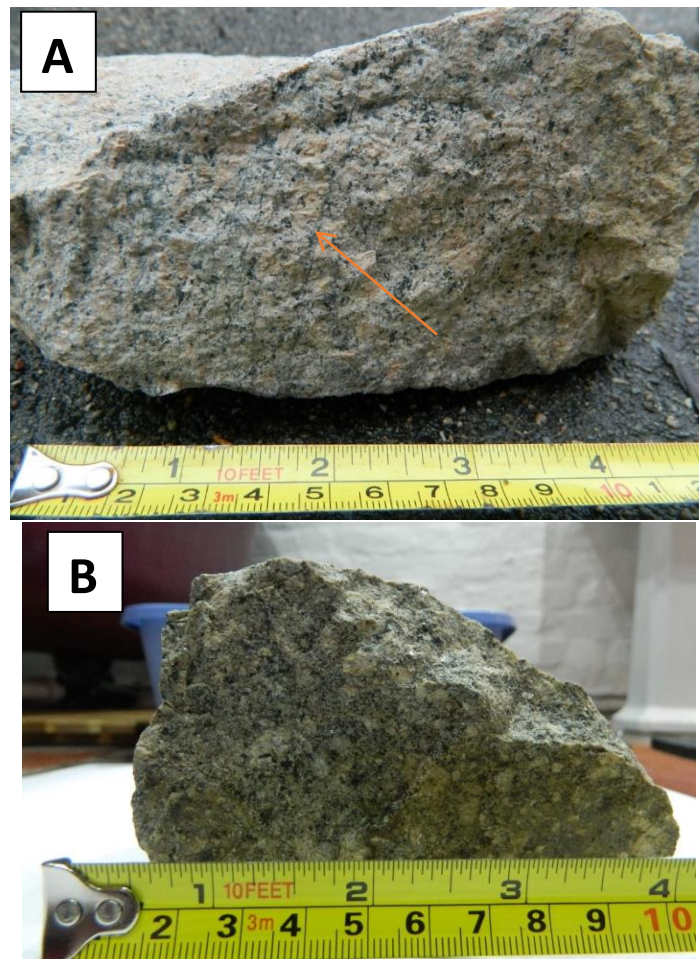
Figure 27: Photographs of the porphyritic microgranite. A: Taken from site 3 (Camlough quarry), showing tuffisite veins (red arrow). B: Sample 6, site 3.
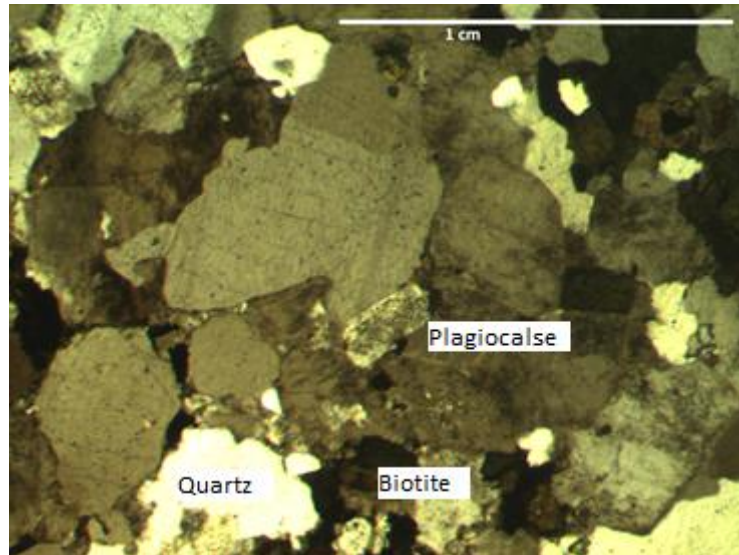
Figure 28: Thin section photograph of sample 6, site 3 (crossed polars) showing crystals of quartz, plagioclase and biotite.

5.6 Forkill Breccias

The Forkill breccias used in this study can be found at Site 4 (GPS 080 825), shown in Figure 29, and also within the Forkill quarry (Site 1).

At site 4 the outcrop is approximately 103m long, although it does appear that these breccias continue further down the road in other fields. This site is made up of coarse, mostly pebble sized rounded granite clasts embedded within a finer matrix (Figure 29). These clasts are mostly made of granite (a black/white or red/pink variety), which is shown in Figure 30, although examples of a black fine matrix rock type do occur.

Within the Forkill quarry, small granite inclusions (3-24cm) can be found within the porphyritic rhyolite, generally in close proximity to the basalt rafts.

When comparing the breccias found at the Forkill quarry and at site 4, it can be seen that at the breccia site the pebbles are generally larger. At both sites the black/white granite clasts (probably the Newry granodiorite) occurs most often and is generally found in larger sized pebbles than the red/pink granite clasts.

The hand samples obtained from site 4 show a fine grey matrix with inclusions of the red and white granites. These inclusions are rounded and are somewhat cemented together by the matrix, however they do break apart easily. Some of the hand samples also show a very weathered appearance but they still show the overall same characteristics. The hand sample obtained from the Forkill quarry also shows the same grey matrix with a rounded clast of granite.

As the Forkill breccia hand samples were so fragile, often it was a granite pebble that was sent for thin section analysis therefore the thin sections from both of the sites show large crystals of biotite, quartz and feldspars. In both cases, several of the crystals also show evidence of alteration/corrosion, shown in Figure 31.

Figure 29: Field outcrop at site 4, showing the Forkill breccias, showing the range in size and shapes of rounded pebbles/boulders (highlighted in red).

Figure 30: A: Photograph of sample 9 (site 4), showing a granite clast within the Forkill breccias. B: Photograph of sample 10 (site 4) showing granite clasts within the Forkill breccias. C: Photograph of sample 22 (site 1) showing the grey
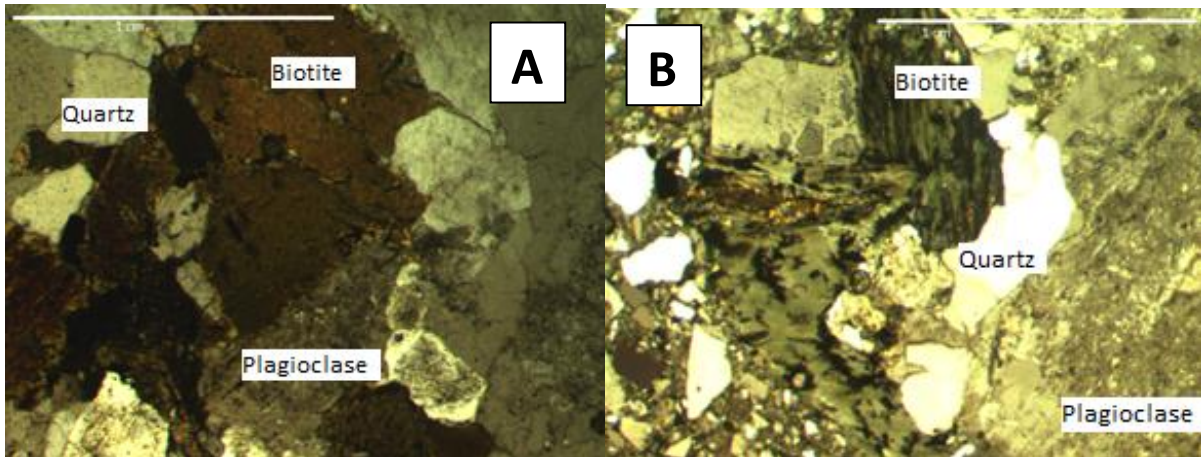
Figure 31: Thin section photographs of the Forkill breccias. A: Sample 10 (site 4), granite clast from the Forkill breccias, showing hydrothermal alteration of crystals (crossed polars). B: Sample 19 (site 1) showing crystals of biotite and of hydrothermally altered plagioclase (crossed polars).

5.7 Central Sheeted Complex

The samples used for the analysis of the central sheeted complex (Site 16) were obtained from various locations on the central sheeted complex of Slieve Gullion. Sample 30 is from a gabbro layer while sample 31 is from a granite layer.

In hand sample the gabbro (Figure 32a) shows a dark black, slightly coarse rock with crystals of biotite and feldspar. The granite hand sample (Figure 32b) shows a pale grey rock that is medium grained.

The gabbro sample obtained for this study was too small to be sent for thin section analysis therefore only the granite has a thin section. This thin section shows a coarse, typical granite however there is evidence of alteration (Figure 33). There is also an example of granophyric texture within this sample.

Figure 32: A: Photograph of sample 30 (Site 16), gabbro from the central sheeted unit. B: Photograph of sample 31 (site 16), granite from the central sheeted unit.
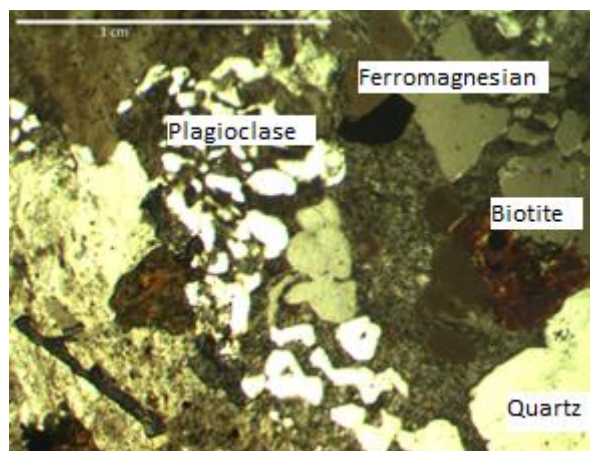
Figure 33: Thin section photograph of sample 31 (site 16), granite from the central sheeted unit showing granophyric texture in plagioclase crystals.

6. Geochemical results

The major element data found in this study is shown in Table 3, for the full geochemical data obtained see appendix A.

For this study only one sample of Newry granite was sent for geochemical analysis. When the major elements found in this study (Table 3) are compared to previously published data (see Table 4) it can be seen that overall they are quite similar. For example, the SiO_2 result for the Newry granite from this study was 69.34% while previous research by Gamble (1982) gives values between 62% and 67%, with one value of 71% and data from Emeleus (1970) gives a value of 63.22% and Richey (1932) gives values of 62.08% and 64.6%.

The Silurian metasediments were sent for geochemical analysis however as they are not volcanic in origin they have not been included in any of the classification graphs. The major element data shows that there are no major chemical differences between the metasediments samples, regardless of which site the samples were taken from.

When comparing the major element data obtained for this study to previously published data it can be seen that in general the porphyritic rhyolite data shows very few differences, apart from the values obtained for Fe_2O_3. The values for this element from this study range from 2.19% to 8.91% while the published values from Patterson (1952/1953) and Emeleus (1961-63) are 1.52% and 1% respectively.

The data obtained for the porphyritic microgranite shows a similar trend to the porphyritic rhyolite as generally all of the values from this study are similar to those previously published, apart from the Fe_2O_3. Again the value obtained for this study (4.14%) is higher than the previously published data (1.62% from Emeleus, 1970 and Patterson 1952/53). This is also the case for CaO as the result obtained for this study is 1.74% while the results obtained by Patterson (1952/53) and Emeleus (1961-1963) were both 0.27%.

 For the Forkill breccias, two samples (sample 10 and 19) from two different sites were sent for geochemical analysis. There are three noticeable differences between the major element results for these two sites. The first of these is the SiO_2 result. In the breccia exclusive site this value is 64.74% while in the Forkill quarry this value is 70%. CaO and TiO_2 also show this difference with the Forkill quarry value being higher than the breccia exclusive site. The remaining major elements are all generally very similar.

The basalt samples studied here are both from the same site and their major element analysis shows that they are chemically very similar, with the biggest difference being in the CaO and sample 1 has a value of 9.07% while sample 3 has a value of 5.3%. Wallace et al. (1994) provide geochemical data for

the lower basalt formation, an intermediate lava at the top of the lower basalts, the Causeway tholeiite member, tholeiitic andesite within one of the Causeway tholeiite flows and the upper basalt formation. Wallace et al. (1994) provide their own data from the basalts in County Antrim as well as previous samples from Lyle (1980, 1985; cited in Wallave et al. 1994). Table 5 shows the average for the main oxides of Wallace et al. (1994) data as well as the three basalt samples from this study. As can be seen in this table, samples 1 and 3 are generally similar to the averages of Wallace et al. (1994). The most notable difference is the K_2O result from sample 3 which is significantly higher than the averaged results. These differences are likely due to contamination from newer rocks and/or alteration from hydrothermal activity from $CaCO_3$ veins in the sample.

The major element data obtained for the gabbro of the central sheeted complex for this study shows great variation to that published by Gamble (1979). The SiO_2 value for this study was 47.96% while Gamble's ranged from 32.31% to 36.21%. The CaO and MgO also varied greatly with 12.37% for the CaO from this study while Gamble's ranged from 0.18% to 0.23% and 8.9% for the MgO from this study while Gamble's ranges from 27.52% to 36.83%. The data obtained for the microgranite of the central sheeted complex is very similar to the data published by Patterson (1952/53) for the same rock unit.

Sample number	Rock Type	SiO_2	Al_2O_3	Fe_2O_3	MnO	MgO	CaO	Na_2O	K_2O	TiO_2	P_2O_5
1	Basalt	48.16	16.78	9.8	0.149	4.85	9.07	2.03	0.29	1.438	0.12
2	Rhyolite	70.8	12.52	3.37	0.071	0.21	1.06	2.96	5.72	0.264	0.03
3	Basalt	53.38	15.63	7.54	0.089	5.9	5.3	2.16	3.17	0.808	0.17
4	Rhyolite	54.86	16.3	8.91	0.144	2.61	5	4.47	2.89	1.196	0.51
5	Rhyolite	74.67	12.54	2.92	0.047	0.26	0.69	3.3	5.28	0.235	0.02
6	Microgranite	70.42	13.56	4.14	0.085	0.56	1.74	3.28	5.42	0.454	0.09
7	Metasediments	72.56	11.7	4.45	0.051	1.81	0.67	1.04	3.24	0.82	0.16
8	Metasediments	64.18	15.85	6.9	0.062	2.46	1.45	2.47	2.94	0.919	0.1
10	Forkill Breccia	70.41	14.73	3.03	0.046	1.02	1.4	3.77	3.94	0.391	0.16
11	Rhyolite	75.82	12.25	2.83	0.03	0.14	0.29	3.12	5.42	0.229	0.06
13	Metasediments	65.36	15.84	6.22	0.061	0.23	1.49	3.76	6.09	0.618	0.15
14	Rhyolite	65.31	16.06	4.3	0.087	2.06	1.75	4.67	3.06	0.731	0.29
16	Rhyolite	74.79	13.1	2.19	0.032	0.1	0.56	3.45	5.44	0.242	0.03
19	Forkill Breccia	64.74	14.22	3.92	0.058	1.84	3.07	3.38	3.49	0.608	0.27
21	Metasediments	55.67	12.9	6.41	0.104	4.49	9.76	1.88	3.35	0.798	0.18
23	Granite	76.02	10.61	4.83	0.057	1.45	1.45	2.39	1.81	0.854	0.16
24	Rhyolite	73.28	12.34	2.94	0.057	0.08	0.77	3.38	5.31	0.213	0.02
26	Metasediments	67.2	15.46	4.5	0.081	2.23	1.62	4.43	2.88	0.641	0.15
27	Metasediments	53.07	17.75	9.95	0.127	4.05	1.51	3.04	5.81	1.334	0.05
29	Rhyolite	78.62	10.76	2.05	0.023	0.04	0.11	3.3	4.59	0.129	0.02
30	Central complex gabbro	47.96	16.91	10.36	0.162	8.9	12.37	2.06	0.25	0.701	0.08
31	Central complex granite	70.37	13.13	4.42	0.075	0.79	1.65	3.41	4.89	0.681	0.16
32	Newry granite	69.34	15.05	3.05	0.055	1.36	2.23	3.94	3.36	0.409	0.14

Table3: Main oxides obtained of all rock samples used in this study. While the Silurian metasediments have been included in this table, they have not been included on the classification graphs.

Rock Type	Source	SiO_2	Al_2O_3	Fe_2O_2	MnO	MgO	CaO	Na_2O	K_2O	TiO_2	P_2O_0
Porphyritic microgranite	Emeleus 1970	71.91	13.42	1.62	0.08	0.27	0.84	3.65	5.49	0.07	0.07
Newry granodiorite	Emeleus 1970	63.22	15.94	1.71	0.04	2.87	4.19	3.88	2.89	0.88	0.29
Unmodified Newry granodiorite	Gamble 1982	65.5	16.52	2.11	0.04	2.41	0.93	4.58	3.32	0.78	-
		65.3	16.3	2.13	0.07	2.62	4.16	4.28	3.31	0.8	-
		71.3	15.35	0.43	0.06	1.3	2.16	3.58	3.19	0.36	-
		65.2	16.63	1.39	0.08	2.47	3.62	4.61	3.23	0.75	-
		65.28	16.35	2.47	0.07	2.21	3.65	4.94	3.24	0.72	-
Newry granodiorite modified in tertiary times	Gamble 1982	67.75	15.83	1.57	0.06	1.85	3.47	4.62	3.2	0.54	-
		65.86	16.05	1.72	0.08	2.43	3.31	4.67	3.5	0.73	-
		65.6	15.45	1.66	0.07	1.5	3.81	4.54	3.23	0.67	-
		65.51	15.91	3.77	0.09	1.69	3.52	4.83	2.87	0.6	-
		66.67	15.64	3.36	0.07	1.44	2.97	4.03	3.23	0.52	-
Hybrid rocks derived from Newry granodiorite	Gamble 1982	62.48	14.5	3.83	0.16	2.47	5.08	3.59	2.92	1.08	-
		62.71	15.76	4.58	0.09	3.1	5.24	3.77	2.59	0.65	-
		66.39	15.95	3.54	0.08	2.13	0.74	3.36	4.78	0.52	-
		62.89	14.87	5.84	0.12	2.44	4.33	3.57	3.01	0.68	-
Porphyritic microgranite	Patterson 1952/1953	71.91	13.42	1.62	0.07	0.27	0.84	3.65	5.49	0.07	0.07
Porphyritic rhyolite	Patterson 1952/1953	74.66	12.62	1.52	0.04	0.31	0.66	3.62	5.02	0.16	0.05
Central complex granite	Patterson 1952/1953	72.06	13.06	1.16	0.02	0.43	1.42	3.81	5.46	0.36	0.09
Porphyritic rhyolite	Emeleus 1961-63	74.66	12.62	1.52	0.04	0.31	0.66	3.62	5.02	0.16	0.05
		76.91	11.79	1	0.04	trace	0.68	3.33	4.98	0.16	0.02
Newry Granodiorite	Richey 1932	64.6	14.64	6.04 (+FeO)		2.8	3.16	4.02	3.15		
		62.08	15.92	7.72 (+FeO)		2.16	5.52	3.34	2.19		
Gabbro	Gamble 1979	36.21			-	39.28	0.18				
		34.67			0.54	36.83	0.18				
		32.31			0.74	27.52	0.18				
Dolerite		34.81			0.44	38.34	0.23				

Table 4: Summary of main oxide information from rocks in the area from different authors.

	SiO2	Al2O3	Fe2O3	MnO	MgO	CaO	Na2O	K2O	TiO2	P2O5
Lower basalt formation	44.7	14.75	12.64	0.176	10.31	9.22	2.14	0.27	1.66	0.18
Causeway tholiite member	51.41	14.62	11.02	0.19	6.53	10.81	2.51	0.49	0.99	0.12
Upper basalt formation	45.55	14.78	11.92	0.17	11.85	9.73	1.95	0.24	1.09	0.11
Sample 1	48.16	16.78	9.8	0.149	4.85	9.07	2.03	0.29	1.438	0.12
Sample 3	53.38	15.63	7.54	0.089	5.9	5.3	2.16	3.17	0.808	0.17

Table 5: Average main oxide results adapted from Wallace et al. (1994) from basalts from the Antrim Coast and basalt data from this study (Samples 1 and 3).

The major element data obtained for this study was then plotted in the IUGS classification and Ewart (1982) tectonic environment classification graphs.

On the IUGS geochemical classification graph (Figure 34), the Newry Granodiorite (sample 32) plots as a granodiorite and on the tectonic environment classification graph (Figure 35) it plots within the high-K calc-alkaline series. The thin section for this sample (figure 13) shows the expected textural characteristics of a granite. However, there is a lot of corrosion of the crystals. This may be due to hydrothermal alteration which is evident throughout the ring dyke complex and surrounding rocks. It is also possible that the newer rocks may have affected the Newry granite.

When plotted on the IUGS geochemical classification graph, the porphyritic rhyolite samples used in this study (samples 2, 4, 5, 16 and 24), mostly plot in the rhyolite category. However, sample 4 plots in the basaltic trachyandesite category. This is likely to be because this rock has undergone alteration, supported by the presence of fractures in the outcrop, and a red/orange tinge to the hand sample suggesting that fluids may have been able to percolate through the fractures. When plotted in the Ewart (1982) tectonic environment classification graph all of the porphyritic rhyolite samples plot within the alkaline series.

The geochemical results for the porphyritic microgranite (sample 6) plot the sample within the granite category on the IUGS classification graph. On the tectonic environment classification graph, the geochemical data plots the porphyritic microgranite sample within the alkaline series.

When plotted on the IUGS classification graph, the samples of the Forkill breccias plot as a granite (sample 10) and a granodiorite (sample 19). These samples plot as the high-K calc-alkaline series on the tectonic environment classification graph.

When looking at the basalts studied here, the IUGS classification graph plots sample 1 as a basalt and sample 3 as a basaltic trachyandesite. When the geochemical data is plotted on the tectonic

environment classification graph, samples 1 falls into the calc-alkaline series, while sample 3 falls into the alkaline series. When the averages of the basalt data from Wallace et al. (1994) previous research are plotted onto the IUGS graph (Figure 36) they plot in the basalt and picro-basalt categories. As the basalt samples from this study show some chemical similarities to those of Wallace et al. (1994) it has been assumed that they are of a similar age (55 to 62Ma, Table 1), however as can be seen in figure 65, the basalts from this study do not plot in the same rock name classifications.

The gabbro sample for this study (sample 30) plots as a gabbro on the IUGS classification, while the granite sample (sample 31) plots as a granite. When plotted on the tectonic environment graph, sample 30 plots just within the calc-alkaline series, while sample 31 plots within the alkaline series.

When looking at the tectonic classification graph (Figure 64) it can be seen that overall the majority of the rock samples studied fall into the high-K calc-alkaline series, which suggests a continental rift origin, or in the alkaline series which suggests a cratonic area which corresponds with the opening of the Atlantic Ocean. Only one sample (sample 23) falls into the calc-alkaline series, which is thought to represent a subduction zone origin, which would correspond with the europium anomaly found in the rare earth elements (see figures 37A, B, C, D), however this sample is not thought to be related to the ring dyke complex.
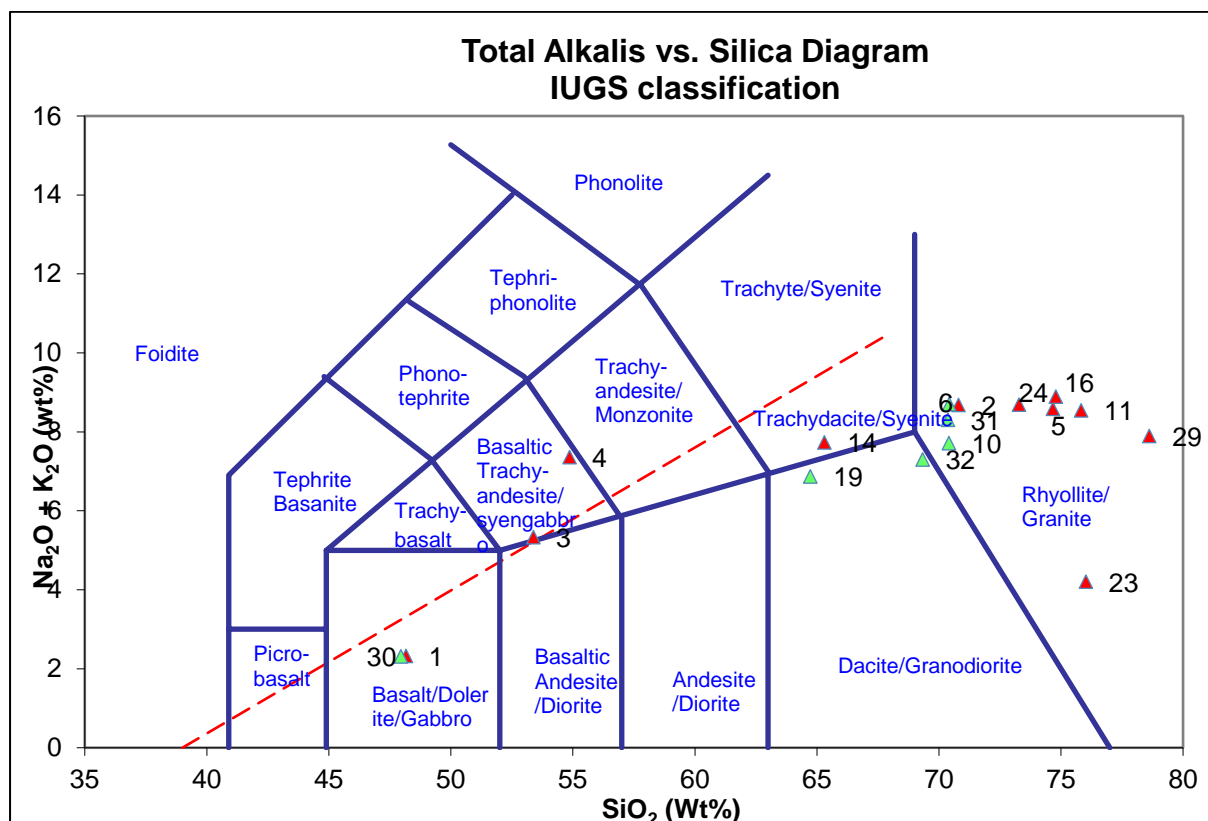
Figure 34: IUGS geochemical classification graph with all data plotted (metasediments excluded). Red points represent extrusive rocks, green points represent intrusive rocks.
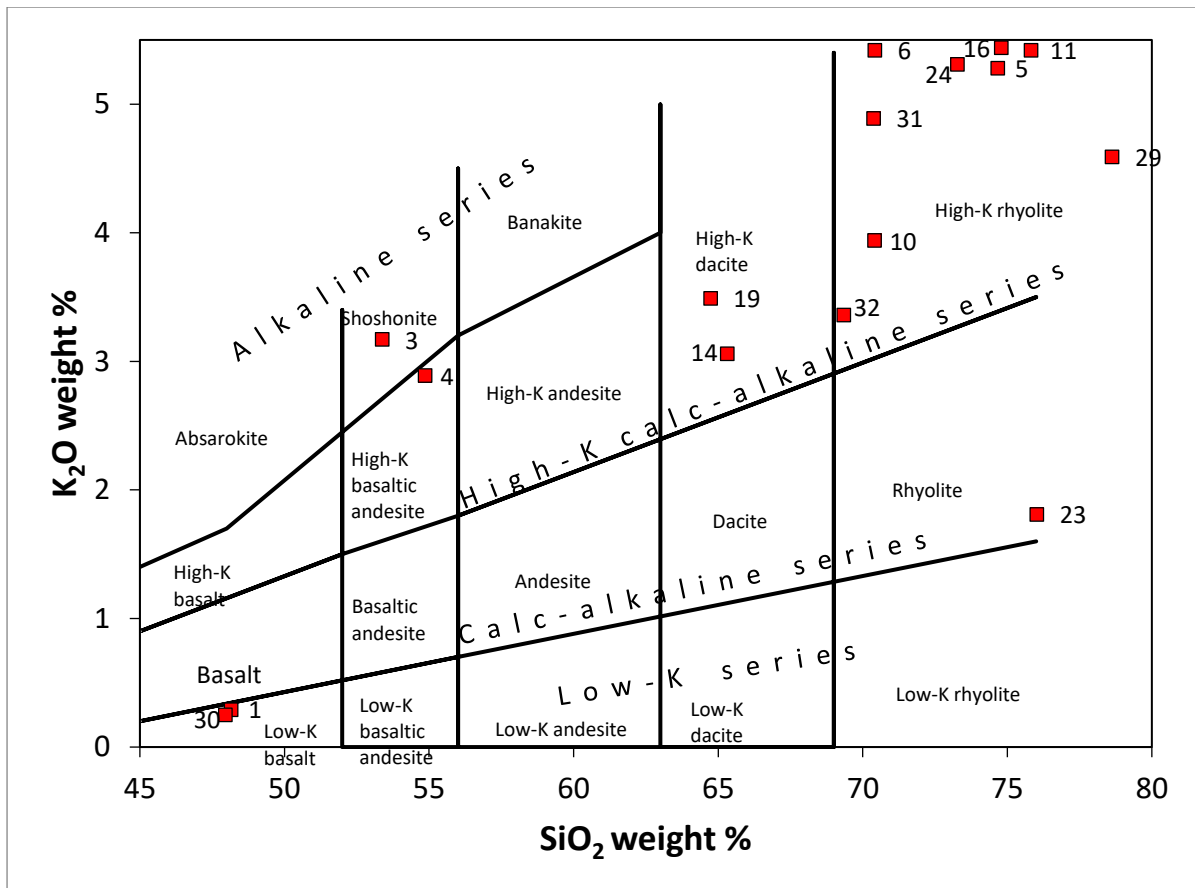
Figure 35: Ewart (1982) Tectonic environment classification graph with all data plotted (metasediments excluded).
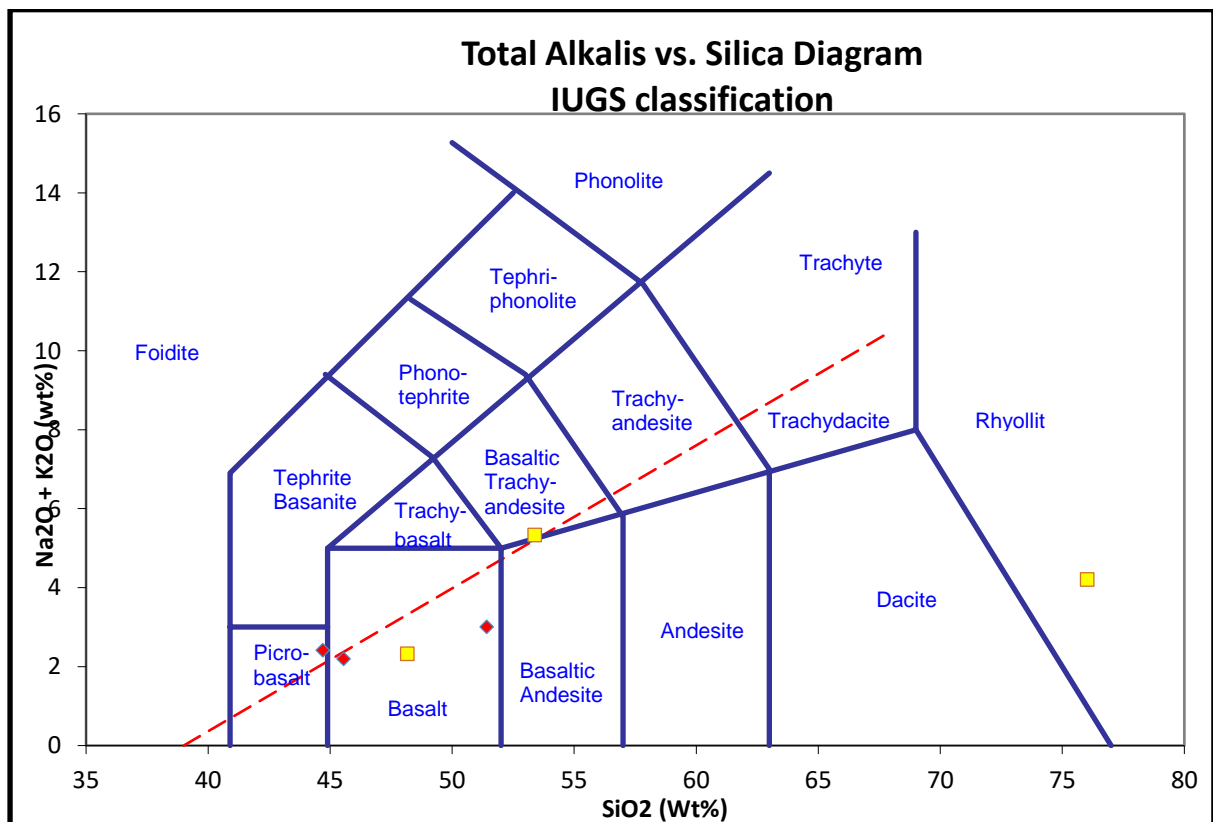
Figure 36: IUGS classification graph with basalt data from this study (yellow points) and from Wallace et al. (1994) (red points).

When looking at the rare earth element graphs (figure 37), it can be seen that the majority of the samples have a depleted europium concentration in comparison with the other elements (only 6 of the samples used in this study do not show this trend). This is known as a negative europium anomaly and is thought to be related to arc magmatism/subduction zones. The basalts, the Forkill breccias and the Newry Granodiorite studied here do not or only very slightly show the Eu anomaly while the porphyritic rhyolite and the porphyritic microgranite, in most cases, show the Eu anomaly very strongly. Within the central complex, the gabbro sample does not show the Eu anomaly whereas the granite sample does. The metasediments studied here also all show the Eu anomaly, although this varies from a slight anomaly to a large anomaly.
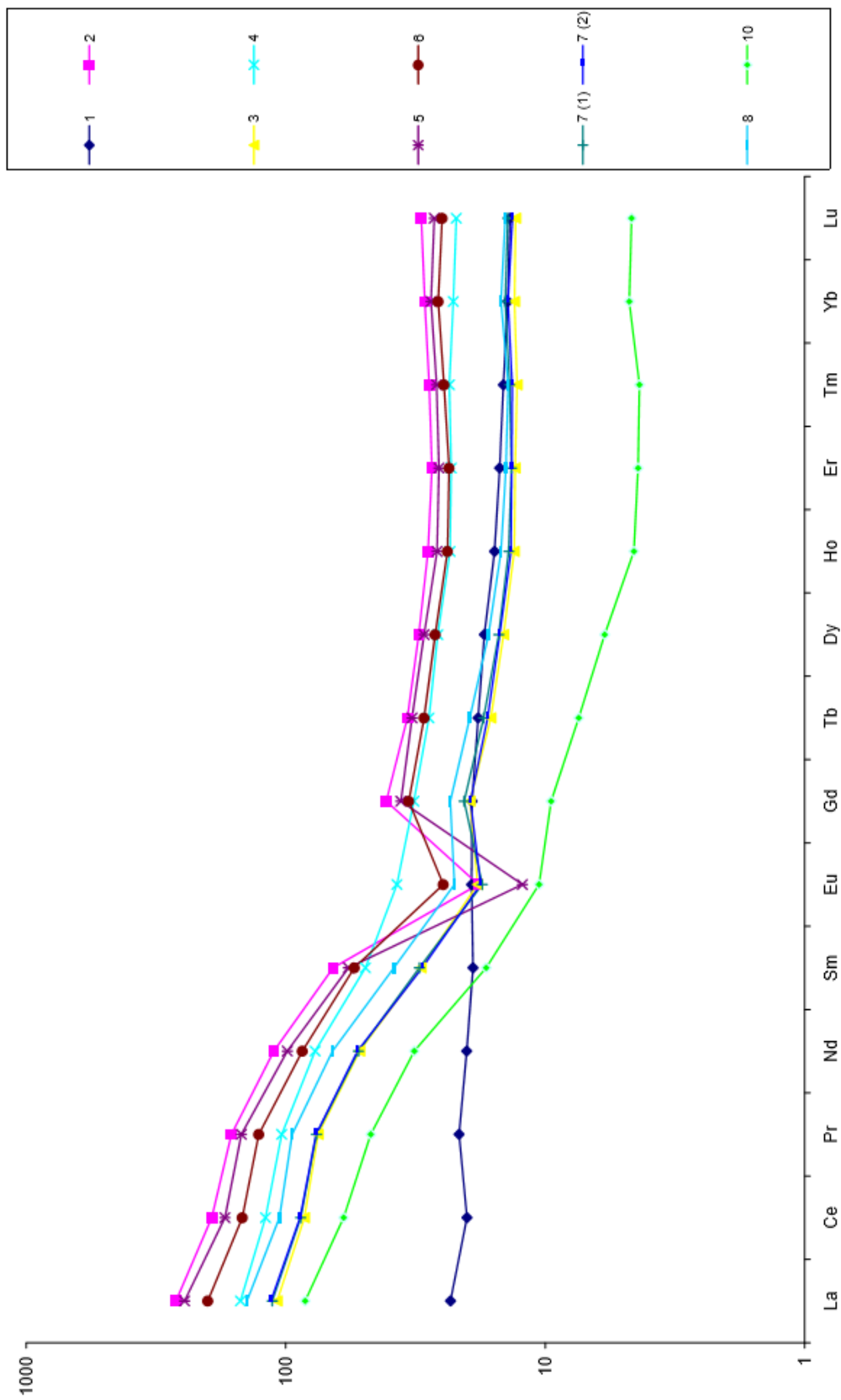
Figure 37A: Rare earth element graph showing samples 1, 2, 3, 4, 5, 6, 7, 8 and 10.
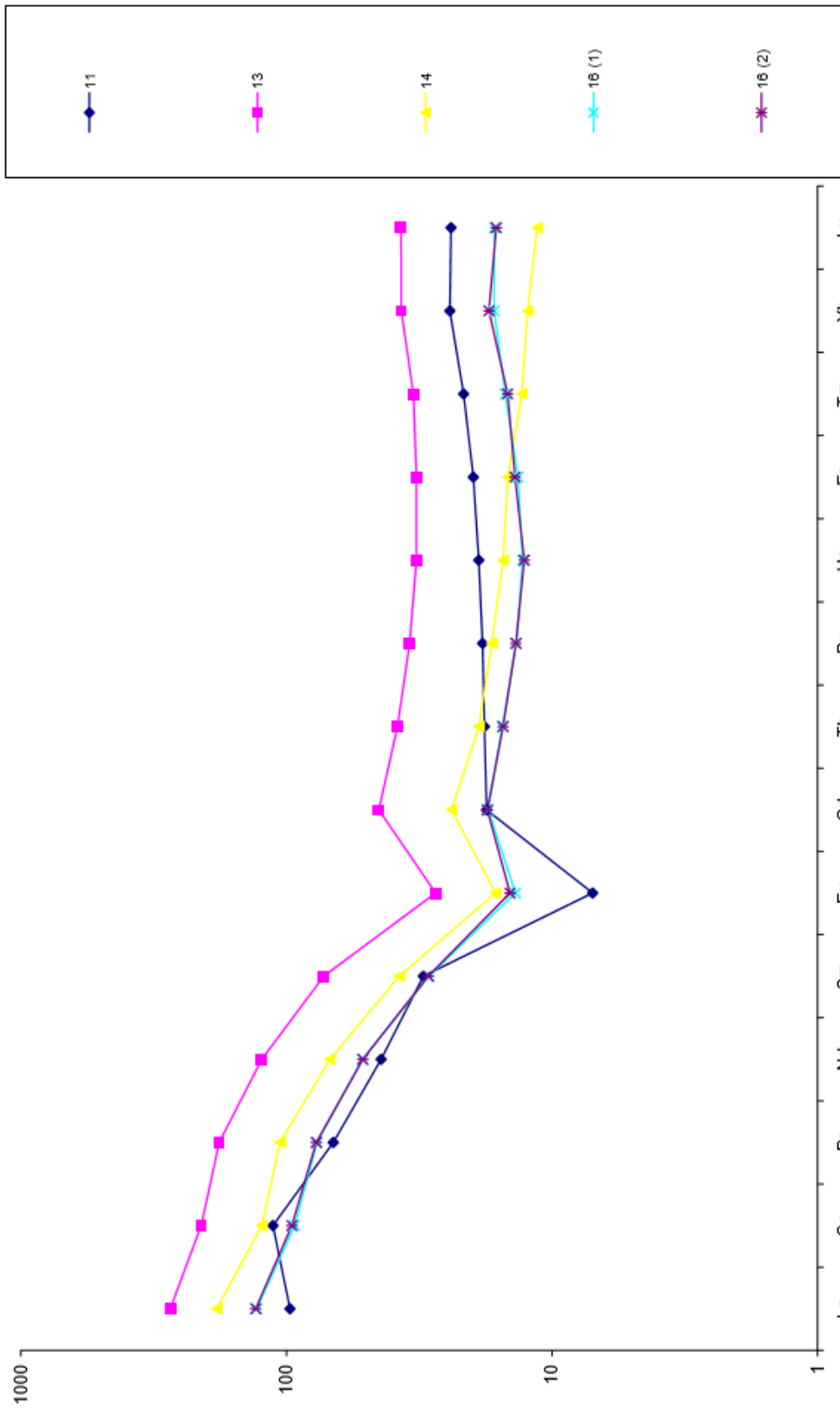
Figure 37B: Rare earth element graph showing samples 11, 13, 14 and 16
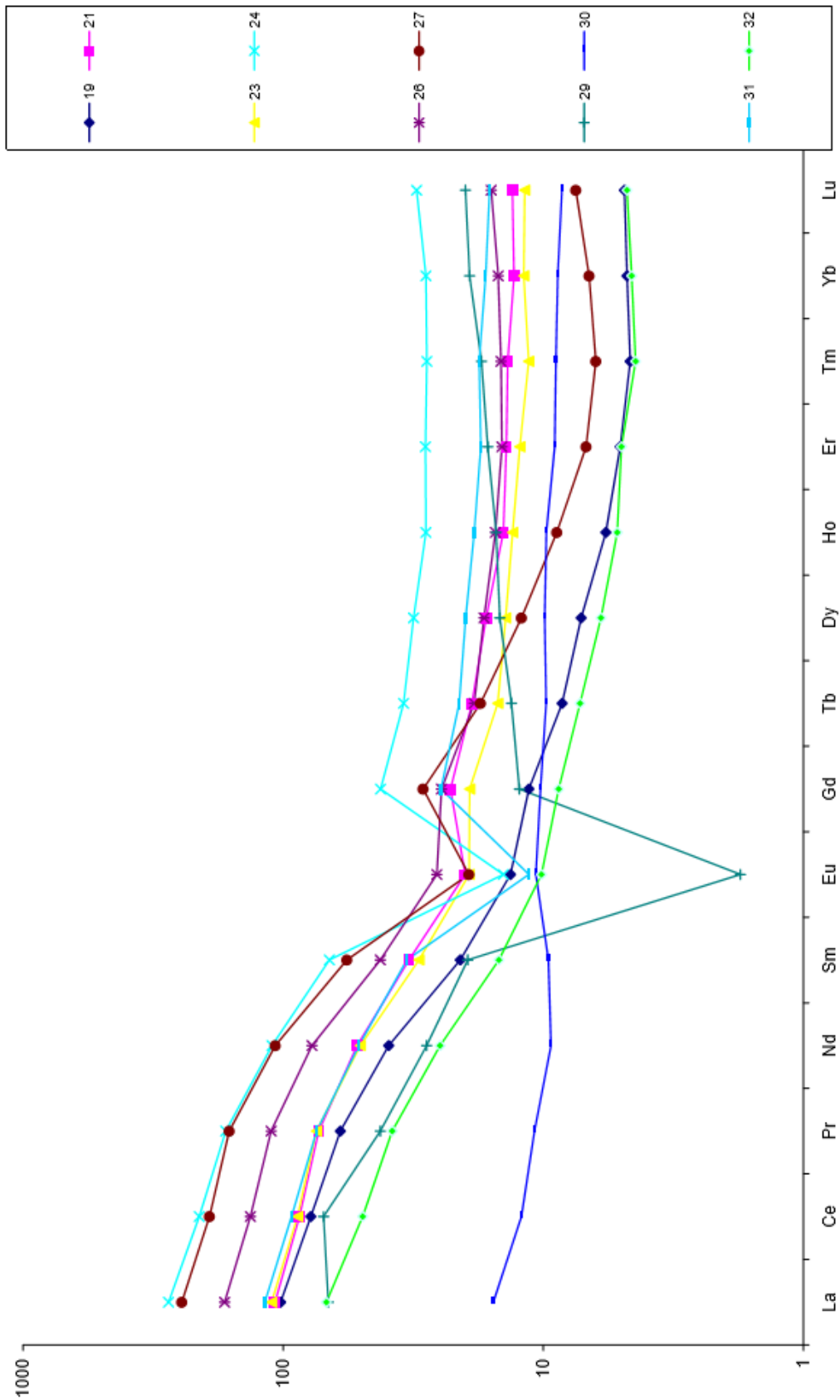
Figure 37C: Rare earth element graph showing samples 19, 21, 23, 24, 26, 27, 29, 30, 31 and 32.
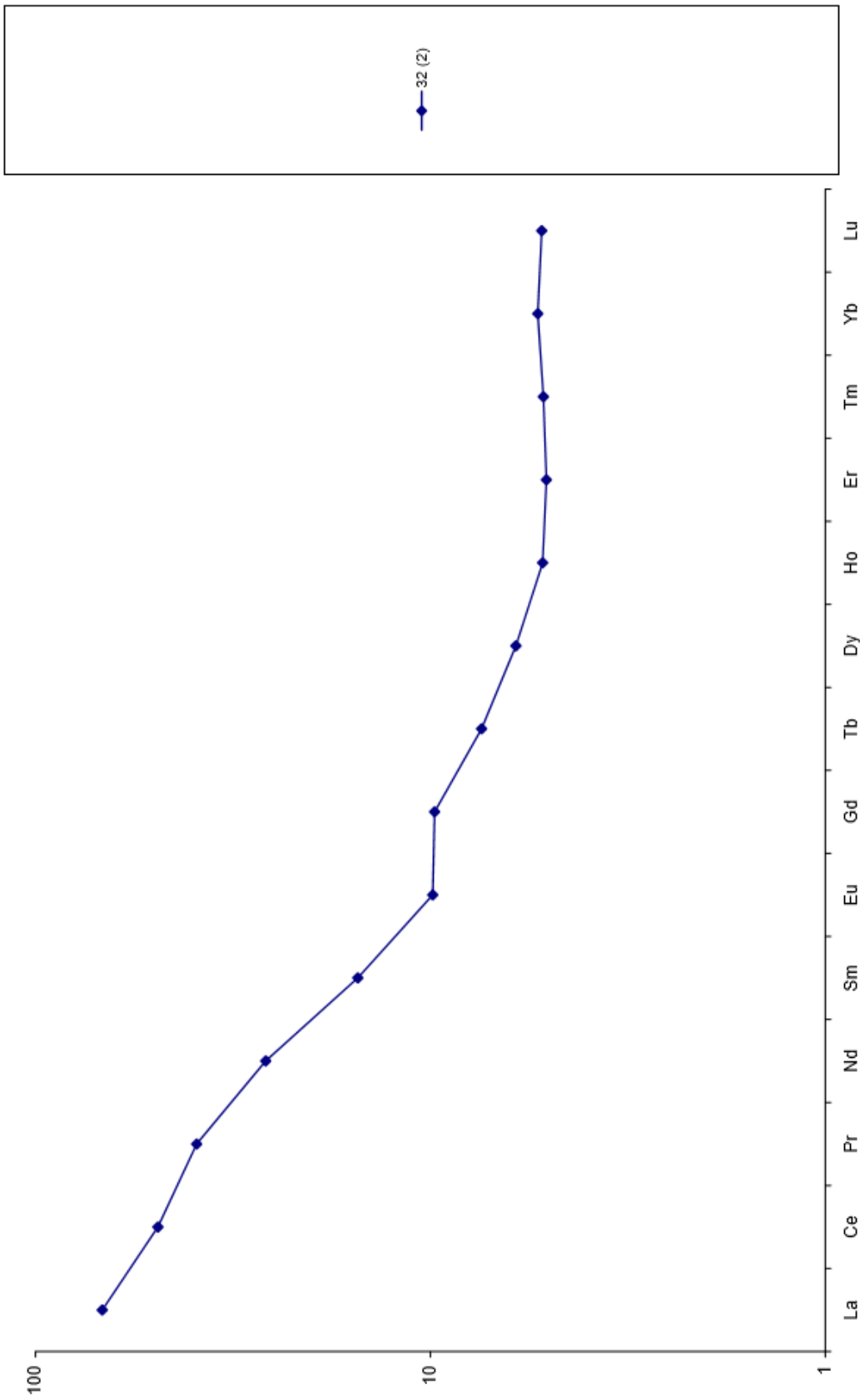
Figure 37D: Rare earth element graph showing sample 32.

Using a combination of the geochemical data and thin section analysis each sample studied here has been given a specific name based on the IUGS classification graph and analysis of the thin sections to provide information regarding the texture of the rock samples (i.e. intrusive or extrusive origin). This information is shown in Table 6 along with the site information and approximate age (based on previous literature).

Sample	Site	Site Name	Rock Name	~ Age
1	1	Forkill Quarry	Basalt	64-59Ma
2	1	Forkill Quarry	Rhyolite	62-58Ma
3	1	Forkill Quarry	Basaltic trachyandesite	64-59Ma
4	2	Ballynamadda Road	Basaltic trachyandesite	62-58Ma
5	2	Ballynamadda Road	Rhyolite	62-58Ma
6	3	Camlough Quarry	Granite(Microgranite)	62-58Ma
7	3	Camlough Quarry	Metasediments*	Silurian
8	3	Camlough Quarry	Metasediments*	Silurian
9	4	Forkill Breccias	N/A	62-58Ma
10	4	Forkill Breccias	Granite	62-58Ma
11	5	Cashel Road 1	Rhyolite	62-58Ma
12	5	Cashel Road 1	N/A	62-58Ma
13	6	Cashel Road 2	Metasediments*	Silurian
14	7	Cashel Road 3	Trachydacite	62-58Ma
15	8	Glassdrumman Pier	N/A	
16	9	Croslieve Mountain	Rhyolite	62-58Ma
17	10	Tievecrom Road	N/A	
18	11	Ravensdale Forest	N/A	
19	1	Forkill Quarry	Granodiorite	62-58Ma
20	1	Forkill Quarry	Metasediments*	Silurian
21	1	Forkill Quarry	Metasediments*	Silurian
23	12	Big Basalt	Microgranite**	64-59Ma
24	13	Forkill House	Rhyolite	62-58Ma
25	3	Camlough Quarry	N/A	62-58Ma
26	3	Camlough Quarry	Metasediments*	Silurian
27	3	Camlough Quarry	Metasediments*	Silurian
28	3	Camlough Quarry	N/A	
29	14	Mullaghbane Golf course	Rhyolite	62-58Ma
30	16	Slieve Gullion Central complex	Gabbro	Younger than ring dyke
31	16	Slieve Gullion Central complex	Microgranite	Younger than ring dyke
32	15	Dublin Road	Granodiorite	Devonian
33	15	Dublin Road	N/A	Devonian

Table 6: List of samples and their corresponding sites, along with the rock name obtained from geochemical and thin section analysis. *Silurian metasediments named from literature. ** microgranite outside the ring dyke complex.

7. Structural Results

The fractures within the three basalt rafts that outcrop in the Forkill Quarry show a preferred orientation of northwest to southeast; however, the remaining two outcrops show a preferred orientation of almost south to west and north-northeast to south-southwest (See Figure 38).

While the porphyritic rhyolite within this quarry is in a large mass, several measurements have been taken (of fractures) from around the quarry to provide a better representation of the site. Half of the recorded outcrops show a preferred orientation of northeast to southwest, while the remaining half show a preferred orientation of northwest to southeast.

Fractures within the porphyritic rhyolite from two other sites around the ring complex broadly show a preferred orientation of northeast to southwest, however one site shows an east to west orientation.

The fractures within the Silurian metasediments within the Forkill quarry do not show a preferred orientation, although each site does show an individual preferred orientation. The Silurian metasediment fracture measurements from the Camlough quarry also show variable preferred orientations.

Measurements of the fiamme structures orientations at two locations in the southwest of the ring complex do both show preferred orientations; however, they are different to each other (north to south and northeast to southwest).

When comparing the rose diagrams created for this study with the orientations of known fault lines (Newry Fault, Southern Uplands Fault, Iapetus Suture etc), some broad conclusions can be made.

The orientations found for the basalts studied show a preferred orientation that is roughly NW-SE which could be considered to coincide with the orientation of the Newry fault; however, there is one result from the rose diagrams of the basalt that shows a NE-SW orientation.

The metasediments structural measurements appear to favour the orientation of the Newry fault line (NW-SE). However, the orientations are still very varied and also show a secondary orientation of NE-SW.

When looking at the rose diagram results obtained for the porphyritic rhyolite samples it can be seen that at all sites, the fracture orientations favour the NE-SW strike, coinciding with the major faults that carry on to Scotland. However, the rose diagrams also show a large proportion of NW-SE orientations as a secondary orientation. This could suggest that the porphyritic rhyolite has been affected by both of these fault systems. When all of the structural ring dyke measurements for the ring dyke rocks alone

are placed into a rose diagram, it shows a preferred orientation of NE-SW with a secondary orientation of NW-SE, suggesting that the ring dyke rocks have been more affected by the NE-SW fault lines, which is the regional trend observed in the area (Figure 5).

When looking at the contour diagrams it can be seen that for the Silurian metasediments the measurements are mostly well orientated however there is one diagram from the Forkill Quarry that shows that the orientations are not as well orientated. For the porphyritic rhyolite measurements, it can be seen that at all sites (Croslieve mountain, site 2 and Forkill Quarry) the measurements are quite well orientated with only one diagram (within the Forkill Quarry) that is not so well orientated. The measurements for the basalts found within the Forkill Quarry are mostly quite well orientated however again there is one diagram that shows that it is not well orientated. The contour diagram for the Newry granodiorite also shows that the measurements are well orientated. In general, it can be seen that the majority of the measurements at all of the sites and from all of the rock types are well orientated suggesting that the fractures found were formed by the same processes at the same time.

Overall it can be seen that the rocks studied have been greatly altered and fractured by tectonic activity in the area. This is further reinforced by the presence of folds within the older Silurian metasediments.

Structural data

Rose Diagrams

Forkill Quarry, Site 1

Basalts
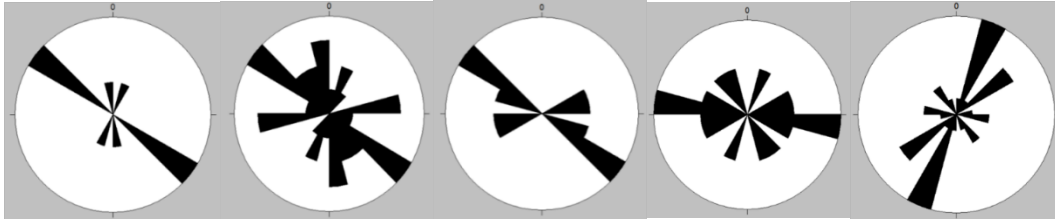
Porphyritic Rhyolite
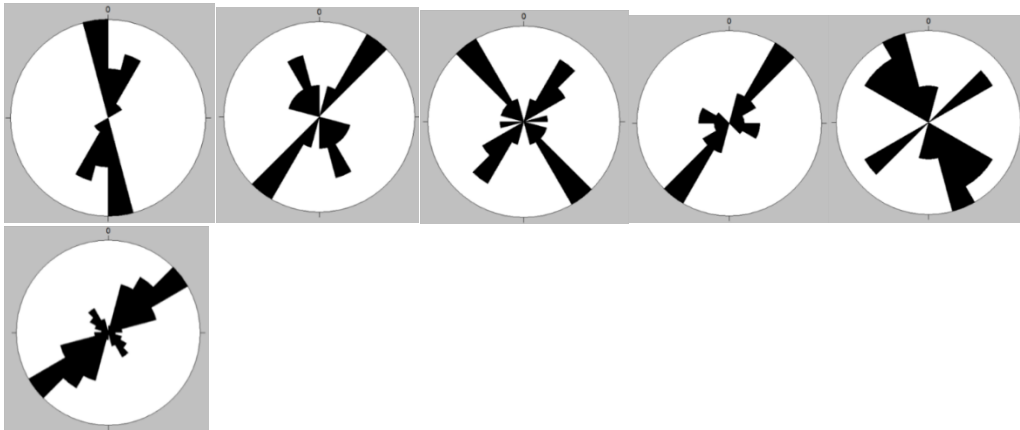
Silurian metasediments
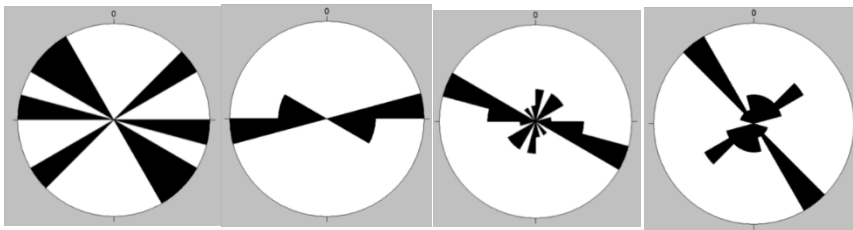
Camlough Quarry, Site 3
Silurian Metasediments
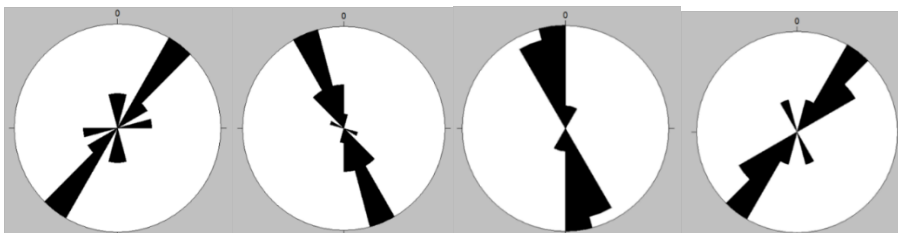
Figure 38A: Structural data plotted in rose diagrams for site 1 and site 3.

Porphyritic Rhyolite Sites

Croslieve Mountain, Site 9   Golf course, Site 14   Site 2
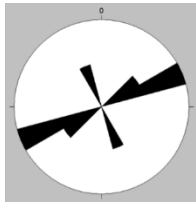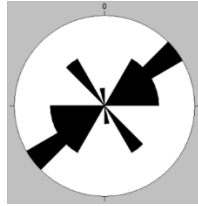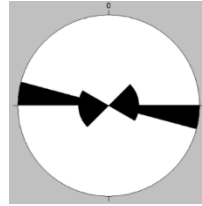
Forkill Quarry, Site 1, all ring dyke rocks
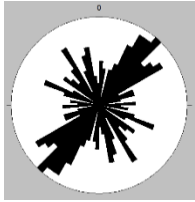
All ring dyke rocks from all sites
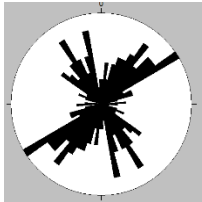
All Silurian metasediment samples from all sites
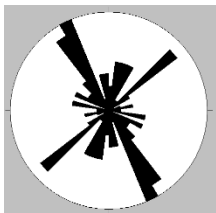
Figure 38B: Rose diagrams for site 9, site 14, site 2 and for specific rock units.

Contour maps

Camlough Quarry, site 3, metasediments
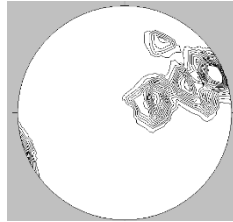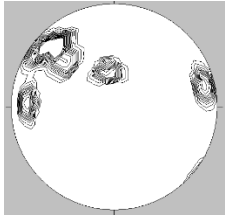
Fiamme Orientations in Porphyritic Rhyolite

Croslieve mountain, site 9   **Mullaghbane golf course, site 14**
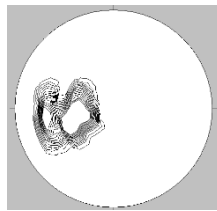
Porphyritic Rhyolite

Croslieve Mountain, Site 9   **Golf course, site 14**   **Site 2**
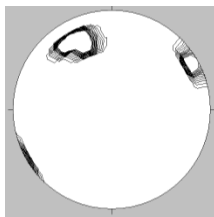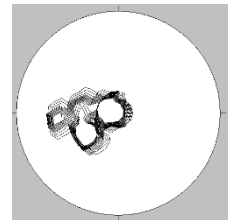
Forkill Quarry, site 1

Basalts
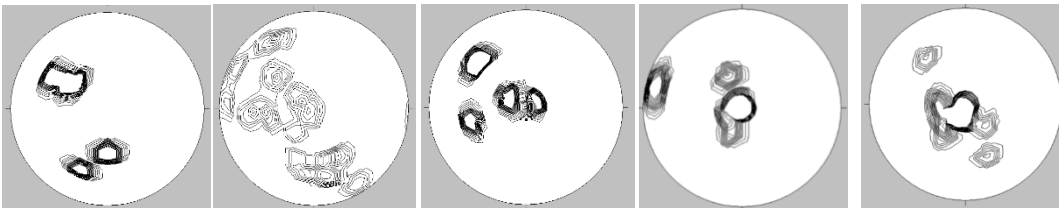
Porphyritic Rhyolite
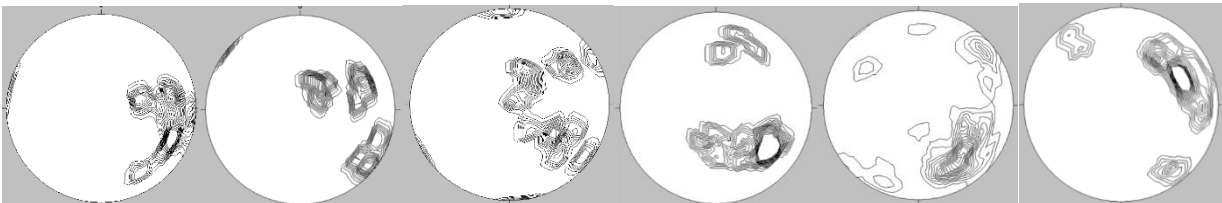
Figure 38C: Contour maps for sites 1 and 3 and for specific rock units.

Silurian metasediments
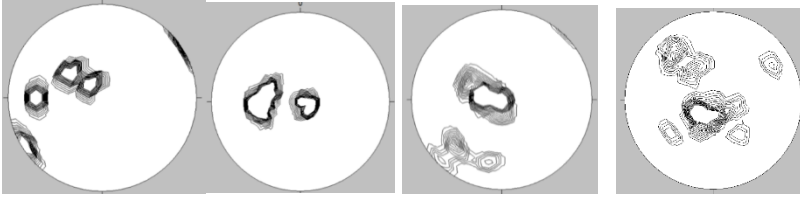
Newry Granite, site 15
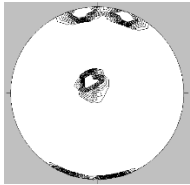
Forkill Quarry, Site 1 – all ring dyke rocks
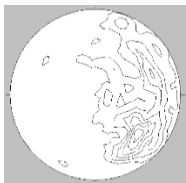
All ring dyke rocks from all sites

All metasediments from all sites
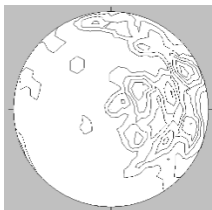
Figure 38D: Contour maps for specific rock units

8. Stratigraphic Sequence

The following proposed stratigraphic sequence of the rock units within the Slieve Gullion ring dyke complex from the older to the youngest unit is based upon sequences proposed by previous literature along with the field work and results obtained for this study.

The oldest unit within this complex is the bedrock, made of the Silurian metasediments, consisting of bands of coarse sandstones and shales. In several places used for this study it can be seen that the metasediments are extremely crushed, especially in those locations that are close to contacts with other rock units associated with the ring complex structure. Within the Forkill Quarry several examples of folding can be seen within the metasediments suggesting that this unit has undergone large amounts of tectonic deformation. Within the Camlough Quarry inclusions of granite and tuffisites can be found suggesting that it has further undergone change due to percolating hot fluids. In this same quarry there is also evidence of a metamorphic change where the sediments are in contact with the porphyritic microgranite, in the form of a colour change. This overall suggests that this is one of the older units as it has been affected by more geological processes.

The second unit within this complex is the Newry granodiorite which is suggested to have intruded the Silurian metasediments. The outcrops of this unit are extremely fractured suggesting that this unit has undergone a lot of tectonic activity. The thin sections for this unit also show several altered/corroded crystals, mainly feldspars, which once again suggests that this is an older unit that has been affected by several processes (tectonic and hydrothermal alteration).

It is suggested here that the third unit of this ring dyke complex is a basalt unit. As the basalt occurs mainly as rafts within the porphyritic rhyolite within the Forkill Quarry, with no obvious source, it is suggested that they have been moved from somewhere else during the emplacement of the porphyritic rhyolite. Spherical inclusions both observed in the hand samples and within the thin sections suggest two modes of emplacement. The roundness of the inclusions on the hand samples could suggest a subaerial origin however the thin section shows that the inclusions are far more coarse than the matrix therefore suggesting an intrusive origin (fragments of reworked gabbro). Overall it is suggested that these rafts were transported during the emplacement of the porphyritic rhyolite, however whether they were formed below the surface and transported up with the rhyolite or they were already on the surface and 'fell' into the ring fracture is unclear. As the basalts in this study (samples 1 and 3) are geochemically similar to those studied by Wallace et al. (1994) it is assumed that they are related and are therefore of a similar age (62-58Ma). This would mean that they could have been formed just prior to ring dyke emplacement.

The next unit of this complex is suggested to be the ring dyke itself (porphyritic rhyolite and porphyritic microgranite). Within the porphyritic rhyolite there are granite inclusions which are thought to be fragments of the Forkill breccias which may have either been transported by the pophyritic rhyolite or may have intruded the porphyritic rhyolite after ring dyke emplacement. As previously mentioned the basalt found within the porphyritic rhyolite has been picked up from an older source during emplacement. The geochemistry of the rhyolite samples generally falls within the rhyolite category on the classification graphs which suggests that this unit has not been altered or contaminated. However, the thin sections show some corroded crystals and what look to be reaction rims around some crystals. This may be an aspect of the rhyolite picking up other material during emplacement. In some locations the porphyritic rhyolite is extremely fractured and shows a preferred orientation which indicates the direction of emplacement. The geochemistry of the porphyritic microgranite produces an expected rock name and the thin sections show little or no alteration/corrosion. As the geochemistry for both the porphyritic rhyolite and the porphyritic microgranite produce expected rocks it can be thought that these are newer units as they have not been altered or contaminated. Within the porphyritic microgranite there are also examples of tuffisites (also found in the Silurian metasediments), suggesting that the tuffisites themselves were produced either during ring dyke emplacement or just after.

The Forkill breccias within this complex are suggested to have occurred during ring dyke emplacement, either at the same time as the emplacement of the rhyolite or before, due to the presence of the breccias within the porphyritic rhyolite in the Forkill quarry. The shape (rounded) and size (pebbles) of the clasts within the Forkill breccias suggests that these are a reworked material cemented together by the fine matrix. In hand sample it is easy to break these breccias apart as they are not completely cemented, suggesting that the matrix was cool/cooling when they formed. They also show evidence of crushing. The thin section analysis of these breccias shows alteration/corrosion of crystals further suggesting that these 'pebbles' are reworked. The geochemistry of these breccias however does give an expected rock name for these samples suggesting that they are not that altered, further supporting that the matrix was cool/cooling when they formed.

The last unit of this complex is the central sheeted unit of Slieve Gullion itself. Both the hand samples and the thin sections show little or no alteration or corrosion and the geochemistry produces rock names that are to be expected. This enforces that this is the youngest unit as it has not undergone any alteration (hydrothermal or contamination).

9. Discussion

Stevenson et al. (2008) originally suggested that due to a lack of contacts and little fabric evidence the porphyritic rhyolite and the porphyritic microgranite of the ring dyke complex were emplaced as separate events under different emplacement models, neither of which could be explained by the traditional ring dyke emplacement model. They therefore suggested that the porphyritic rhyolite was therefore an ignimbrite sheet while the porphyritic microgranite was a laccolithic intrusion. However, both Troll et al. (2008) and Emeleus et al. (2012) disagreed with Stevenson et al. (2008) as they supported the traditional ring dyke model, involving caldera subsidence creating a ring fault and subsequent magma infill creating the ring dyke. Emeleus et al. (2012) used their own field, petrographic and geochemical data to define the complex as a ring dyke and further suggested that the AMS anisotropy measurements proposed by Stevenson et al. (2008) are difficult to interpret and can often be chaotic due to magma emplacement. Both Troll et al. (2008) and Emeleus et al. (2012) also report examples of sharp contacts within the ring dyke complex as well as crush zones at the contacts. This study has also found examples of sharp contacts between the porphyritic rhyolite and the Silurian metasediments at the Forkill Quarry; and between the porphyritic microgranite and the Silurian metasediments at the Camlough Quarry supporting the model of Emeleus et al. (2012).

The orientations of the fractures within the outcrops studied show strong correlations with major regional faults that traverse the area. The metasediment structural measurements show a strong orientation of NW-SE which corresponds with the orientation of the Newry Fault, however there is a secondary orientation that is perpendicular to this (NE-SW) which corresponds with the Southern Uplands Fault (SUF). The basalts rafts studied here also show a strong orientation that corresponds with the Newry Fault (NW-SE). The measurements obtained for the porphyritic rhyolite show a strong orientation of NE-SW which corresponds with the SUF, however once again there is a secondary orientation that is perpendicular (NW-SE, which corresponds with the Newry Fault). When looking at all of the structural measurements for the ring dyke as a whole is can be seen that the favoured orientation is NE-SW (SUF) with a secondary perpendicular orientation of NW-SE (Newry Fault).

The majority of the rock samples studied here fall into the alkaline series or the high-K calc-alkaline series when the geochemistry data are plotted on the tectonic environment graph (Figure 64) which represents a cratonic environment and a continental rift environment respectively. This supports that this complex is related to the opening of the Atlantic Ocean. It is also possible that the Tertiary magmas may have incorporated crust that was formed during the closure of the Iapetus (Silurian/Devonian) which may have affected some of the results obtained here.

10.   Conclusions

This study used a combination of detailed field observations, mapping, structural measurements, thin section analysis and geochemical analysis to study the various rock units within the Slieve Gullion ring dyke complex and to re-evaluate emplacement models and overall several conclusions can be made.

Geochemical data from this study is generally very similar to data previously published by previous authors.

When the basalt geochemistry data from this study was compared to Antrim basalt data published by Wallace et al. (1994) it can be seen that they are chemically very similar therefore it has been assumed that they are of a similar age (55-62 Ma) which places the basalts found in this study as older than the ring dyke or the same age as it.

When looking at the IUGS classification graph it can be seen that the majority of the samples fall into the 'expected' rock name categories however there are a few samples that fall into categories that were not expected. This is likely due to either hydrothermal alteration or weathering of the sample.

When the geochemical data was plotted into the Ewart (1982) tectonic environment classification graph the majority of the samples fall into the high-k calc-alkaline series or in the alkaline series. This corresponds with the opening of the Atlantic Ocean and the mantle plume activity.

The rare earth element graphs show that the majority of the samples have a depleted europium concentration (also known as a negative europium anomaly) which is thought to be related to arc magmatism/subduction zones i.e. at the time of the closure of the Iapetus. While the majority of the samples show this anomaly, it is the porphyritic rhyolite and the porphyritic microgranite that most strongly show this trend suggesting there is a greater degree of crustal contamination in these magmas.

The structural measurements show that the fractures measured at all sites and for all rock types are well orientated which suggests that they have been greatly altered by tectonic activity in the area.

The suggested order of emplacement for the Slieve Gullion ring dyke complex units is therefore: 1) Silurian metasediments; 2) Newry granodiorite 3) Basalts; 4) Ring dyke rocks (porphyritic rhyolite and porphyritic microgranite); 5) Forkill breccias; and 6) Central sheeted complex.

This study has found that there are several examples of clear contacts between the different rock units as well as evidence of crushing and percolating hot fluids (tuffisites) therefore this study supports the traditional ring dyke emplacement model for the emplacement of these rocks as suggested by Emeleus et al. (2012).

References

Bell, B.R. (1994) Picritic basalts from the Palaeocene lava field of west-central Skye, Scotland: evidence for parental magma compositions. *Mineralogical Magazine*. 58. 347-356

Bell, B.R., Claydon, R.V., Rogers, G. (1994) The Petrology and Geochemistry of Cone-Sheets from the Cuillin Igneous Complex, Isle of Skye: Evidence for Combined Assimilation and Fractional Crystalisation during Lithospheric Extension. *Journal of Petrology.* 35. 1055-1094.

Berlo, K., Tuffen, H., Smith, V.C., Castro, J.M., Pyle, D.M., Mather, T.A., Geraki, K. (2013) Element variations in rhyolitc magma resulting from gas transport. *Geochemica et Cosmochimica Acta.* 121. 436-451.

Bell, B.R., Emeleus, C.H. (1988) A review of silicic pyroclastic rocks of the British Palaeogene Volcanic Province. *Geological Society Special Publication.* 39. 365 – 379.

Brooks, M. (1973) Some aspects of the Palaeogene Evolution of Western Britain in the context of an underlying mantle hot spot. *The Journal of Geology.* 81. 81-88.

Cloos, H. (1941) Bau und Tatigkeit von Tuffschloten*. Geologische Runddschau.* 32. 709-800.

Cooper, M.R., Anderson, H., Walsh, J.J., Van Dam, C.L., Young, M.E., Earls, G., Walker, A. (2012) Palaeogene Alpine tectonics and Icelandic plume-related magmatism and deformation in Northern Ireland. *Journal of the Geological Society.* 169. 29-36.

Dagley, P., Mussett, A.E. (1986) Palaeomagnetism and radiometric dating of the British Palaeogene Igneous Province: Muck and Eigg. *Geophysical Journal International*. 85. 221-242.

Dagley, P., Mussett, A.E., Skelhorn, R.R. (1987) Polarity, stratigraphy and duration of the Palaeogene igneous activity of Mull, Scotland. *Journal of the Geological Society*. 144. 985-996.

Dicken, A.P., Jones, N.W. (1983) Isotopic evidence for the age and origin of pitchstones and felsites, Isle of Eigg, NW Scotland. *Journal of the Geological Society.* 140. 691-700

Emeleus, C.H. (1962) The Porphyritic Felsite of the Palaeogene Ring Complex of Slieve Gullion, Co. Armagh. *Proceedings of the Royal Irish Academy.* 62. 55-76.

Emeleus, C.H., Troll, V.R., Chew, D.M., Meade, F.C. (2012) Lateral versus vertical emplacement in shallow-level intrusions? The Slieve Gullion Ring-complex revisited. *Journal of the Geological Society.* 169. 157-171.

Ewart, A., (1982) The mineralogy and petrology of Tertiary-Recent orogenic volcanic rocks: with special reference to the andesitic-basaltic compositional range; p. 25-95 in, Thorp, R.S., ed., Andesites: Orogenic Andesites and Related Rocks, John Wiley and Sons, New York, 724 p.

Galland, O., Holohan, E., van Wyk de Vries, B., Burchardt, S. (2015) Laboratory Modelling of Volcano Plumbing Systems: A Review. 1-68.

Gamble, J.A. (1979) The Geochemistry and Petrogenesis of Dolerites and Gabbros From the Palaeogene Central Volcanic Complex of Slieve Gullion, North East Ireland. *Contributions to Mineralogy and Petrology.* 69. 5-19.

Gamble, J.A., Meighan, I.G., McCormick, A.G. (1992) The petrogenesis of Palaeogene microgranites and granophyres from the Slieve Gullion Central Complex, NE Ireland. *Journal of the Geological Society.* 149. 93-106.

Gamble, J.A., Wysoczanski, R.J., Meighan, I.G. (1999) Constraints on the age of the British Palaeogene Volcanic Province from ion microprobe U-Pb (SHRIMP) ages for acid igneous rocks from NE Ireland. *Journal of the Geological Society*. 156. 291-299.

Ganerod, M., Smethurst, M.A., Torsvik, T.H., Prestvik, T., Rousse, S., McKenna, C., van Hinsbergen, D.J.J., Hendriks, B.W.H. (2010) The North Atlantic Igneous Province reconstructed and its relation to the Plume Generation Zone: the Antrim Lava Group revisited. *Geophysical Journal International.* 182. 183-202.

Garfunkel, Z., Katz, A. (1967) New magmatic features in Makhtesh Ramon, Southern Israel. *Geological Magazine.* 104. 608-629.

Geldmacher, J., Haase, K.M., Devey, C.W., Garbe-Schonberg, C.D. (1998) The Petrogenesis of Palaeogene cone-sheets in Ardnamurchan, NW Scotland: petrological and geochemical constraints on crustal contamination and partial melting. *Contributions to Mineralogy and Petrology.* 131. 196- 209.

Geyer, A., Marti, J. (2014) A short review of our current understanding of the development of ring faults during collapse caldera formation. *Frontiers in Earth Science*. 2 .22.

Herrero-Bervera, E., Walker, G.P.I, Canon-Tapia, E., Garcia, M.O. (2001) Magnetic fabric and inferred flow direction of dikes, conesheets and sill swarms, Isle of Skye, Scotland. *Journal of Volcanology and Geothermal Research*. 106. 195-210.

Hitchen, K., Ritchie, J.D. (1993) New K-Ar ages, and a provisional chronology, for the offshore part of the British Palaeogene Igneous Province. *Scottish Journal of Geology.* 29. 73-85.

Holness, M.B., Isherwood, C.E. (2003) The aureole of the Rum Palaeogene Igneous Complex, Scotland. *Journal of the Geological Society*. 160. 15-27.

Kennedy, B., Jellinek, A.M., Stix, J. (2008) Coupled caldera subsidence and stirring inferred from analogue models. *Nature Geoscience.* 1. 385-389.

Kolzenburg, S., Heap, M.J., Lavalee, Y., Russell, J.K., Meredith, P.G., Dingwell, D.B. (2012) Strength and permeability recovery of tuffisite-bearing andesite. *Solid Earth.* 3. 191-198

McDonnall, S., Troll, V.R., Emeleus, C.H., Meighan, I.G., Brock, D., Gould, R.J. (2004) Intrusive history of the Slieve Gullion ring dyke, Co.Armagh, Ireland: implications for the internal structure of silicic subcaldera magma chambers. *Mineralogical Magazine.* 68. 725-738.

Meade, F.C., Chew, D.M., Troll, V.R., Ellam, R.M., Page, L.M. (2009) Magma Ascent along a Major Terrane Boundary: Crustal Contamination and Magma Mixing at the Drumadoon Intrusive Complex, Isle of Arran, Scotland. *Journal of Petrology.* 50. 2345-2374.

Meade, F.C., Troll, V.R., Ellam, R.M., Freda, C., Font, L., Donaldson, C.H. and Klonowska, I., 2014. Bimodal magmatism produced by progressively inhibited crustal assimilation. *Nature communications*, *5*.

Meade, F.C., Troll, V.R., Ganerod, M. In: 58th Annual Irish Geological Research Meeting (2015): Rewriting the stratigraphy of the British and Irish Palaeogene Igneous Province: A short-lived explosive episode in NE Ireland. Abstract page 6/7

Meighan, I.G., Gibson, D., Hood, D.N. (1984) Some aspects of Tertiary acid magmatism in NE Ireland. *Mineralogical Magazine.* 48. 351-361.

Meighan, I.G., McCormick, A.G., Gibson, D., Gamble, J.A., Graham, I.J. (1988) Rb-Sr isotopic determinations and the timing of Palaeogene central complex magmatism in NE Ireland. In Gamble, J.A., Meighan, I.G., McCormick, A.G. (1992) The Petrogenesis of Palaeogene microgranites and granophyres from the Slieve Gullion Central Complex, NE Ireland. *Journal of the Geological Society.* 149. 93-106.

Meighan, I.G., Fallick, A.E., McCormick, A.G. (1992) Anorogenic granite magma genesis: new isotopic data for the southern sector of the British Palaeogene Igneous Province. *Transactions of the Royal Society of Edinburgh.* 83. 227-233

Patterson, E.M. (1953) Petrochemical Data for Some Acid Intrusive Rocks from the Mourne Mountains and Slieve Gullion. *Proceedings of the Royal Irish Academy.* 55. 171-188.

Pearson, D.G., Emeleus, C.H., Kelley, S.P. (1996) Precise ^{40}Ar/^{39}Ar age for the initiation of Palaeogene volcanism in the Inner Hebrides and its regional significance. *Journal of the Geological Society*. 153. 815-818.

Reynolds, D.L. (1951) The geology of Slieve Gullion, Foughill and Carrickarnan: an actualistic interpretation of a Palaeogene gabbro/granophyre complex. *Transactions of the Royal Society of Edinburgh.* 62. 86-142.

Richey, J.E., Thomas, H.H. (1932) The Palaeogene ring complex of Slieve Gullion, Ireland. *Quart journ geol soc.* 88. 776-849.

Saunders, A. D., Fitton, J. G., Kerr, A. C., Norry, M. J. and Kent, R. W. (1997) The North Atlantic Igneous Province, in Large Igneous Provinces: Continental, Oceanic, and Planetary Flood Volcanism. American Geophysical Union, Washington, D. C.

Smith, S., & Roberts, C. (1997). The Geology of Lundy. *Lundy Field Society.*

Stevenson, C.T.E., O'Driscoll, B., Holohan, E.P., Couchman, R., Reavy, R.J., Andrews, G.D.M. (2008). The structure, fabrics and AMS of the Slieve Gullion ring-complex, Northern Ireland: testing the ring dyke emplacement model. *Geological Society Special Publications*. 302. 159-184.

Thorpe, R.S., Tindle, A.G., Gledhill, A. (1990) The Petrology and Origin of the Palaeogene Lundy Granite (Bristol Channel, UK). *Journal of Petrology.* 31. 1379-1406.

Troll, V.R., Chadwick, J.P., Ellam, R.M., McDonnell, S., Emeleus, C.H., Meighan, I.G. (2005) Sr and Nd isotope evidence for successive crustal contamination of Slieve Gullion ring dyke magmas, Co. Armagh, Ireland. *Geological Magazine.* 142. 659-668.

Walker, G.P.L. (1975) A new concept of the evolution of the British and Tertiary intrusive centres. *Journal of the Geological Society*. 131. 121-141.

Wallace, J.M., Ellam, R.M., Meighan, I.G., Lyle, P., Rogers, N.W. (1994) Sr isotope data for the Palaeogene lavas of Northern Ireland: evidence for open system petrogenesis. *Journal of the Geological Society.* 151. 869-877.

Appendix A: Results from geochemical analysis for the rock samples used in this study.

	SiO2	Al2O3	Fe2O3(T)	MnO	MgO	CaO	Na2O	K2O	TiO2	P2O5	LOI	Total
1	48.16	16.78	9.8	0.149	4.85	9.07	2.03	0.29	1.438	0.12	8.08	100.8
2	70.8	12.52	3.37	0.071	0.21	1.06	2.96	5.72	0.264	0.03	1.44	98.44
3	53.38	15.63	7.54	0.089	5.9	5.3	2.16	3.17	0.808	0.17	5.57	99.71
4	54.86	16.3	8.91	0.144	2.61	5	4.47	2.89	1.196	0.51	1.36	98.26
5	74.67	12.54	2.92	0.047	0.26	0.69	3.3	5.28	0.235	0.02	0.61	100.6
6	70.42	13.56	4.14	0.085	0.56	1.74	3.28	5.42	0.454	0.09	0.95	100.7
7	72.56	11.7	4.45	0.051	1.81	0.67	1.04	3.24	0.82	0.16	2.45	98.94
8	64.18	15.85	6.9	0.062	2.46	1.45	2.47	2.94	0.919	0.1	2.23	99.57
10	70.41	14.73	3.03	0.046	1.02	1.4	3.77	3.94	0.391	0.16	0.98	99.88
11	75.82	12.25	2.83	0.03	0.14	0.29	3.12	5.42	0.229	0.06	0.76	100.9
13	65.36	15.84	6.22	0.061	0.23	1.49	3.76	6.09	0.618	0.15	1.16	101
14	65.31	16.06	4.3	0.087	2.06	1.75	4.67	3.06	0.731	0.29	2.02	100.3
16	74.79	13.1	2.19	0.032	0.1	0.56	3.45	5.44	0.242	0.03	0.49	100.4
19	64.74	14.22	3.92	0.058	1.84	3.07	3.38	3.49	0.608	0.27	3.26	98.87
21	55.67	12.9	6.41	0.104	4.49	9.76	1.88	3.35	0.798	0.18	4.82	100.4
23	76.02	10.61	4.83	0.057	1.45	1.45	2.39	1.81	0.854	0.16	0.87	100.5
24	73.28	12.34	2.94	0.057	0.08	0.77	3.38	5.31	0.213	0.02	0.35	98.75
26	67.2	15.46	4.5	0.081	2.23	1.62	4.43	2.88	0.641	0.15	1.48	100.7
27	53.07	17.75	9.95	0.127	4.05	1.51	3.04	5.81	1.334	0.05	1.79	98.48
29	78.62	10.76	2.05	0.023	0.04	0.11	3.3	4.59	0.129	0.02	0.4	100
30	47.96	16.91	10.36	0.162	8.9	12.37	2.06	0.25	0.701	0.08	0.7	100.5
31	70.37	13.13	4.42	0.075	0.79	1.65	3.41	4.89	0.681	0.16	0.81	100.4
32	69.34	15.05	3.05	0.055	1.36	2.23	3.94	3.36	0.409	0.14	0.88	99.82

	Sc	Be	V	Ba	Sr	Y	Zr	Cr	Co	Ni	Cu	Zn
1	43	2	283	45	141	28	82	240	35	70	170	70
2	4	3	12	489	44	53	441	<20	1	<20	20	160
3	19	3	143	348	199	24	145	130	22	90	20	100
4	18	3	122	1348	289	44	364	20	19	40	20	100
5	3	4	14	302	31	58	363	<20	2	<20	<10	100
6	7	3	23	835	78	50	568	20	3	<20	<10	80
7	11	2	76	420	66	26	297	80	12	30	20	110
8	15	2	109	345	178	31	268	110	16	50	<10	110
10	5	3	48	773	347	10	167	30	6	<20	20	70
11	3	3	14	392	40	33	417	50	<1	<20	20	190
13	19	4	8	410	40	64	1234	<20	2	<20	<10	<30
14	9	5	82	794	432	33	212	60	11	20	20	90
16	2	3	8	419	34	25	436	<20	<1	<20	<10	50
19	8	3	67	40	9	20	70	60	18	1	<5	97
21	16	2	107	120	19	70	30	90	17	2	<5	120
23	10	1	68	60	12	30	20	60	13	1	<5	63
24	3	4	7	<20	<1	<20	<10	90	24	2	<5	173
26	11	3	65	70	10	30	<10	140	18	1	<5	82
27	25	3	168	150	29	90	80	1030	33	2	<5	318
29	<1	5	<5	<20	<1	<20	<10	90	25	2	<5	210
30	39	<1	209	370	51	110	150	70	15	2	<5	8
31	9	3	59	<20	8	<20	20	60	19	1	<5	202
32	6	3	46	20	7	<20	10	50	18	1	<5	112

	Ga	Ge	As	Rb	Nb	Mo	Ag	In	Sn	Sb	Cs	La
1	18	1	<5	17	4	<2	1.2	<0.2	1	<0.5	3.5	7.3
2	24	1	<5	180	25	3	4.3	<0.2	4	<0.5	3.3	83.3
3	22	1	<5	129	14	<2	2	<0.2	3	0.6	7.3	34
4	21	<1	<5	50	18	<2	3.3	<0.2	3	<0.5	1.1	47.1
5	23	2	<5	169	21	3	1.6	<0.2	4	<0.5	3	77.3
6	23	2	<5	157	27	<2	2.9	<0.2	3	<0.5	2.9	62.9
7	15	1	<5	116	12	2	2.6	<0.2	2	<0.5	5.1	35.7
8	20	2	<5	139	17	<2	1.9	<0.2	2	<0.5	10	44.5
10	18	2	<5	155	10	<2	1	<0.2	3	<0.5	3.8	26.5
11	25	2	<5	184	24	2	6.5	<0.2	5	<0.5	2.1	30.5
13	24	3	<5	130	33	<2		<0.2	4	<0.5	1.4	86.2
14	23	2	<5	104	11	<2	1.2	<0.2	2	<0.5	1.7	57.6
16	24	2	<5	170	20	<2	3	<0.2	4	<0.5	4.5	41
19	427	15	169	8	<2	<0.5	<0.2	2	<0.5	2.3	793	32.2
21	216	29	173	10	<2	<0.5	<0.2	2	1	4.6	336	33.8
23	166	26	296	11	<2	0.5	<0.2	1	<0.5	1.8	412	34.9
24	29	57	346	19	2	0.7	<0.2	3	<0.5	4.6	355	86.8
26	422	32	397	14	<2	0.7	<0.2	2	<0.5	2.2	1249	52.9
27	137	15	295	30	<2	<0.5	<0.2	3	<0.5	20.1	578	77.2
29	6	32	273	27	3	0.5	<0.2	5	<0.5	4.6	25	21.1
30	203	17	37	3	<2	<0.5	<0.2	<1	<0.5	1	104	4.9
31	113	37	62	21	<2	<0.5	<0.2	4	<0.5	5.7	661	37.1
32	327	14	121	6	<2	<0.5	<0.2	2	<0.5	3.5	699	21.5

	Ce	Pr	Nd	Sm	Eu	Gd	Tb	Dy	Ho	Er	Tm	Yb
1	16.3	2.4	12	3.6	1.39	5	0.9	5.6	1.1	3.2	0.46	2.9
2	157	18.1	66.3	12.6	1.31	10.6	1.7	10	2	5.8	0.9	6.1
3	68.9	8.39	31	5.8	1.31	5.1	0.8	4.7	0.9	2.8	0.41	2.7
4	97.3	11.6	46	9.5	2.69	8.3	1.4	8.4	1.6	4.9	0.75	4.7
5	139	16.6	58.9	11	0.88	9.3	1.6	9.5	1.8	5.5	0.84	5.7
6	120	14.2	51.5	10.4	1.79	8.7	1.4	8.6	1.7	5	0.79	5.4
7	71.4	8.55	31.4	5.8	1.27	5.2	0.8	4.9	1	2.9	0.43	2.9
8	86	10.6	39.4	7.4	1.62	6	1	5.4	1	3	0.44	3.1
10	48.6	5.27	19.1	3.2	0.76	2.5	0.4	1.9	0.3	0.9	0.14	1
11	91.5	7.47	26.3	5.9	0.51	4.6	0.9	5.9	1.3	4.2	0.69	5.1
13	170	20.1	74	13.9	1.98	11.6	1.9	11.2	2.3	6.9	1.06	7.7
14	101	11.9	40.9	7.2	1.18	6.2	0.9	5.5	1.1	3.1	0.42	2.6
16	76.7	8.62	30.9	5.6	1.02	4.5	0.8	4.4	0.9	2.9	0.48	3.5
19	63.7	6.75	23.5	4	0.97	2.9	0.4	2.3	0.4	1.1	0.15	1
21	70.4	8.18	31	6.3	1.44	5.9	0.9	5.4	1	3	0.44	2.7
23	71.5	8.34	30.1	5.8	1.39	5	0.7	4.5	0.9	2.6	0.36	2.5
24	171	18.6	65.9	12.7	1.03	10.9	1.7	10.2	2	6	0.9	5.9
26	109	12.5	46.3	8.1	1.85	6.4	0.9	5.5	1.1	3.1	0.47	3.1
27	156	18	64	10.9	1.39	7.5	0.9	3.9	0.6	1.5	0.2	1.4
29	56.8	4.74	16.8	3.7	0.13	3.2	0.7	4.8	1.1	3.5	0.55	4
30	9.9	1.21	5.6	1.8	0.77	2.7	0.5	3.2	0.7	1.9	0.29	1.8
31	75.5	8.33	30.5	6.4	0.82	6.4	1	6.5	1.3	3.7	0.56	3.5
32	40	4.32	15.3	2.8	0.72	2.4	0.4	2	0.4	1.1	0.16	1

	Lu	Hf	Ta	W	Tl	Pb	Bi	Th	U
1	0.44	2.3	0.2	1	<0.1	<5	<0.4	1	0.2
2	0.97	9.9	1.6	1	0.9	25	<0.4	18.7	4.6
3	0.42	3.8	1	1	0.8	17	<0.4	11	3.1
4	0.71	7.8	1	<1	0.3	15	<0.4	5.1	1.4
5	0.87	7.7	1.8	1	0.8	26	<0.4	18.7	4.1
6	0.81	11.3	1.7	2	0.8	25	<0.4	13.7	2.8
7	0.44	6.8	1	4	0.9	27	<0.4	8.6	9.3
8	0.46	6.5	1.2	2	0.7	41	<0.4	11	2.9
10	0.15	4.1	0.8	<1	0.8	21	<0.4	12	1.6
11	0.78	8.6	1.6	<1	0.9	33	<0.4	18.6	4.7
13	1.2	23.2	1.8	<1	0.9	20	<0.4	13.3	2.7
14	0.37	4.9	0.8	2	0.6	12	<0.4	12.4	3.3
16	0.53	8.1	1.5	<1	0.9	27	<0.4	16.3	3.2
19	0.16	4.1	0.7	<1	0.5	21	<0.4	11.2	3.7
21	0.42	4.9	0.9	2	0.7	17	<0.4	9.8	2.7
23	0.38	7.6	1	<1	0.4	11	<0.4	8.1	2.3
24	0.99	8.8	1.7	1	0.8	25	<0.4	20.6	4.4
26	0.51	10.2	1.1	2	0.6	32	<0.4	14.7	3.8
27	0.24	9.6	1.3	1	1.8	278	0.4	39.3	18.4
29	0.64	9.3	2.4	<1	1.2	32	<0.4	23.4	4.7
30	0.27	1.2	0.2	<1	0.1	<5	<0.4	0.8	0.3
31	0.52	2.3	1.7	<1	0.9	20	<0.4	17.9	3.9
32	0.16	3.2	0.7	<1	0.6	23	<0.4	9.6	3.3